Methyl Dynamics in Proteins from NMR Slowly Relaxing Local Structure Spin Relaxation Analysis: A New Perspective

Eva Meirovitch,*,†ௐ Antonino Polimeno,*,‡ and Jack H. Freed*,§

Faculty of Life Sciences, Bar-Ilan University, Ramat-Gan 52900, Israel, Department of Physical Chemistry, University of Padua, 35131 Padua, Italy, and Baker Laboratory of Chemistry and Chemical Biology, Cornell University, Ithaca, New York 14853-1301

NMR spin relaxation of ^{2}H nuclei in ^{13}CH$_2$D groups is a powerful method for studying side-chain motion in proteins. The analysis is typically carried out with the original model-free (MF) approach adapted to methyl dynamics. The latter is described in terms of axial local motions around, and of, the methyl averaging axis, mutually decoupled and independent of the global motion of the protein. Methyl motion is characterized primarily by the axial squared order parameter, S^2_{axis}, associated with fluctuations of the methyl averaging axis. This view is shown to be oversimplified by applying to typical experimental data the slowly relaxing local structure (SRLS) approach of Polimeno and Freed (*Adv. Chem. Phys.* **1993,** *83,* 89) which can be considered the generalization of the MF approach. Neglecting mode coupling and the asymmetry of the local ordering and treating approximately features of local geometry imply inaccurate values of S^2_{axis}, hence of the residual configurational entropy derived from it. S^2_{axis}, interpreted as amplitude of motion, was found to range from near disorder to almost complete order. Contrary to this picture, we find with the SRLS approach a moderate distribution in the magnitude of asymmetric local ordering and significant variation in its symmetry. The latter important property can be associated implicitly with the contribution of side-chain rotamer jumps. This is consistent with experimental residual dipolar coupling studies and theoretical work based on molecular dynamics simulations and molecular mechanics considerations. Configurational entropy is obtained in the SRLS approach directly from experimentally determined asymmetric potentials. Inconsistency between order parameters from ^{2}H relaxation and from η_{HC-HH} cross-correlation and increase in order parameters with increasing temperature were observed with the MF approach. These discrepancies are reconciled, and physically tenable temperature dependence is obtained with the SRLS approach.

I. Introduction

NMR spin relaxation is an important source of information on motional properties of proteins and their relation to function.[1−5] Backbone dynamics is usually studied using the ^{15}N−^{1}H bond as a probe. Side-chain dynamics, on which we focus in this study, uses the methyl group, which maps out the protein core quite comprehensively.[6−10] Specific isotope-labeling techniques have been developed to produce the probes ^{13}CH$_3$, ^{13}CH$_2$D, and ^{13}CHD$_2$. ^{2}H relaxation in ^{13}CH$_2$D is very useful due to the dominance of the quadrupole interaction and the development of effective pulse sequences.[11−13] Extensive validation of experimental robustness was provided by Millet et al.[12] and Skrynnikov et al.[13] The analysis of ^{13}C relaxation in ^{13}CH$_3$ is complicated by the complexity of the spin system.[14,15] However, through the use of the ^{13}CHD$_2$ isotopomer and appropriate pulse sequences, it has been possible to obtain consistent ^{2}H and ^{13}C relaxation results.[16,17] Experiments that yield the cross-correlated relaxation rate η_{HC-HH} in ^{13}CH$_3$ groups were also developed.[18]

However, several problems outlined below have been encountered with methyl dynamics in proteins. These may stem from experimental imperfections and/or data analysis. In this study we focus primarily on ^{2}H relaxation in ^{13}CH$_2$D groups. As pointed out above, the experimental methodologies for measuring ^{2}H relaxation rates were shown to be robust. Data analysis is usually carried out with the model-free (MF) approach.[19−21] The latter assumes that the local motion of the dynamic probe and the global motion of the protein are decoupled since they occur on different time scales and oversimplifies the local geometry. A simplified spectral density, used to fit the experimental data,[22,23] was suggested. The best-fit parameters include a squared generalized order parameter, S^2, and an effective local motion correlation time, τ_e. For methyl dynamics S^2 was parametrized as $0.1 S^2_{axis}$. $[P_2(\cos 110.5°)]^2 = 0.1$ (with P_2 denoting the Legendre polynomial of rank 2) is associated with the motion *around* the methyl averaging axis, whereas S^2_{axis} is associated with the axial (per definition)[24] motion *of* this axis (to be called below the "axis"). The value of 0.1 corresponds to a tetrahedral angle of 110.5° and an $r_{CH} = r_{CD}$ distance of 1.115 Å. Practically identical results are obtained with 109.5° and $r_{CH} = r_{CD} = 1.135$ Å.[17,18] S^2_{axis} is interpreted as amplitude of motion. Its temperature dependence was found to be unexpectedly small, nearly zero, and in some cases opposite to the expected trend.[25] For many proteins, a three-pronged distribution in S^2_{axis}, with average values on the order of 0.2−0.3, 0.6, and 0.8 on a 0−1 scale, was obtained.[25,26] Within the scope of the "amplitude of motion" concept, the lower S^2_{axis} values reflect unduly large excursions of the "axis"

* Authors to whom correspondence should be addressed. E-mail: eva@nmrsgi1.ls.biu.ac.il; antonino.polimeno@unipd.it; jhf@ccmr.cornell.edu.
† Bar-Ilan University.
‡ University of Padua.
§ Cornell University.

in tightly packed protein cores. The extensive NMR-detected flexibility was not reproduced with molecular dynamics (MD) simulations[24,27] based on traditional methods[28] for calculating S^2. Recent MD studies found that uneven populations of interconverting rotameric states about χ_1 and χ_2 affect significantly the lower S^2_{axis} values[29] and showed that anharmonic effects omitted in the traditional methods[28] must be accounted for to explain NMR-derived order parameters.[30] *J*-coupling and residual dipolar coupling (RDC) studies[31,32] detected uneven populations of rotameric states around χ_1. In some cases, the rates of these motions were found to be slow on the nanosecond time scale of the spin relaxation experiment.[30,32] In other cases, correlation times on the order of nanoseconds were estimated.[13,30,32]

A recent molecular mechanics (MM)-based model has correlated S^2_{axis} with the equilibrium probability distribution, P_{eq}, of rapidly interconverting rotameric states. $P_{eq} = -\exp(u)$, where u represents the local potential. High S^2_{axis} values were associated with a single dominant rotamer, and lower S^2_{axis} values with two or three rapidly interconverting rotamers.[33] Independently, 80 ns MD simulations indicated that in some cases rotameric transitions occur on the subnanosecond time scale, while in others they occur on the time scale of tens of nanoseconds.[33] Variations in the population of rotameric states have been associated with changes in the packing environment.[33] Yet, only weak empirical correlations between S^2_{axis} and the packing density at the methyl site were found by others.[7,27] Likewise, only weak empirical correlations were found between S^2_{axis} and the burial of side chains,[30] their solvent accessibility,[7,27] and other structural properties.[27]

The complexity of the phenomena affecting NMR order parameters, in general, and the influence of rotameric population distributions, in particular, led to the conclusion that methods that predict NMR order parameters from structure should consider which rotamers are accessible and what their weights are.[30] Nonetheless, MF-derived NMR order parameters of both backbones[34] and side chains[35] were interpreted recently for several proteins with considerable success in terms of contact models.

The B1 immunoglobulin binding domain of peptostreptococcal protein L (to be called below "protein L") was studied with both ^{2}H relaxation[12,13] and η_{HC-HH} cross-correlation.[18] At 25 °C similar S^2_{axis} values were obtained with both experiments, albeit with spectral densities featuring different parameter combinations. Above 25 °C S^2_{axis} from η_{HC-HH} was found to *increase* with increasing temperature. At 45 °C S^2_{axis} from η_{HC-HH} exceeded significantly S^2_{axis} from ^{2}H relaxation.[18]

The inconsistencies and inaccuracies mentioned above may stem from the oversimplified nature of the MF approach and its overextension. Thus, the methyl group is taken to be engaged in motion *around* and *of* the "axis", while the original MF formula features a single effective local motion characterized by S^2 and τ_e. To treat methyl dynamics S^2 is set equal to 0.1 S^2_{axis}, while this factorization is only valid in the extreme motional narrowing limit (where $\tau_e \approx 0$), which is exceeded in practice, since τ_e assumes finite values in ^{2}H relaxation analysis. Note that accuracy in the value of S^2_{axis} is particularly important when interpretation of this quantity in terms of residual configurational entropy is pursued.[36−39] The parameter τ_e is associated with motion both *around* and *of* the averaging axis while these processes are assumed to be decoupled and should therefore be associated with different time-scale-separated correlation times. The tilt angles between the various frames,

including the tetrahedral angle, are to enter the calculation through appropriate Wigner rotations. In the MF approach, the tetrahedral angle enters the calculation as the squared order parameter 0.1. As outlined below, this is only justified when τ_e is practically zero. Decoupling of the local (τ_e) and global (τ_m) motions, inherent in the MF approach, is valid when the time scale separation is large *and* the local ordering is either very high or very low.[40,41] Although S^2 values may pertain to the perturbation limit, the time scale separation between τ_e and τ_m might not be large enough to justify the neglect of mode coupling (see below). Finally, there is ample evidence that the local ordering is asymmetric,[29,30−33] contrary to the axial symmetry inherent in the definition of S^2_{axis}.[24]

Notwithstanding the simplifications outlined above, the original MF spectral density adapted to methyl dynamics is often able to fit the ^{2}H T_1 and T_2 relaxation rates with good statistics. However, as generally known and reiterated here, low χ^2 can be obtained with parametrizing entities instead of physically meaningful quantities.[41] The process whereby an oversimplified version of an exact experiment-compatible spectral density yields low χ^2 values but inaccurate best-fit parameters, which have absorbed the deviations from the experimental spectral density, is known as "force fitting".[40,41]

To test the effects of the simplifications outlined above on the results obtained, we analyzed typical experimental methyl relaxation data with the slowly relaxing local structure (SRLS) approach of Freed and co-workers,[42−44] which we applied recently to NMR spin relaxation in proteins.[40,41,45−48] The SRLS approach is a rigorous stochastic model that solves the same physical problem addressed mathematically by the MF approach. It can be considered the generalization of the MF approach, yielding the latter in asymptotic limits. In the SRLS approach, the relative orientations of the magnetic, diffusion, and ordering tensors, which are the quantities that determine restricted motions in liquids, are accounted for rigorously and generally. No restrictions are imposed on the time scale separation between the global and the local motions, and mode coupling is accounted for rigorously. The spatial restrictions at the site of the motion of the methyl group are expressed as asymmetric (or rhombic) local potentials.[40,41,43,44,48]

We showed previously that the original[19,20] and extended[21] MF spectral densities often force-fit the experimental ^{15}N relaxation data.[40,41,45−48] Herein, we apply the SRLS approach to ^{2}H and η_{HC-HH} methyl relaxation data of protein L[12,13,18] and ^{2}H methyl relaxation data of ubiquitin[8] and compare results with those obtained previously[8,13,18] with the MF approach. We find that the SRLS and MF analyses yield significantly different results. A systematic investigation, whereby the SRLS model is enhanced gradually until a consistent physical picture is obtained, shows that *the local potential at the site of the motion of the methyl group is asymmetric or rhombic*. The three-pronged distribution featured by a number of experimental ^{2}H data sets (cf. ref 8) is shown to reflect *different symmetries* of the local potential, with *moderate differences in its strength*. This picture is very different from motional amplitudes clustered in three groups covering a range that extends from near disorder to almost complete order.[25,26] We show that *the same* SRLS spectral density reproduces both ^{2}H relaxation and η_{HC-HH} cross-correlation rates measured at 25 °C for protein L, while the MF analysis used spectral densities featuring different parameter combinations. The η_{HC-HH} rates measured at 45 °C are reproduced with *smaller* ordering than that found to prevail at 25 °C, while the MF approach yielded a physically untenable increase in the local ordering with increasing temperature. The

SRLS/NMR Analysis of Methyl Dynamics in Proteins

J. Phys. Chem. B, Vol. 110, No. 41, 2006 **20617**

deficiencies of the MF analysis are shown to be implied by force fitting.

Our results are consistent with information on side-chain rotamer jumps around χ_1 (and χ_2) provided by *J*-coupling and RDC,[31,32] MD,[30] and MM[33] studies. In these investigations P_{eq} has been associated with S_{axis}^2, the magnitude of which was taken to discriminate between single-rotamer scenarios (high S_{axis}^2) and multirotamer scenarios (low S_{axis}^2). In the SRLS approach P_{eq} is associated with the principal values S_0^2 and S_2^2 of a rhombic local ordering tensor defined in terms of a rhombic local coupling/ordering potential. The latter features an axial term with coefficient c_0^2 and a rhombic term with coefficient c_2^2. P_{eq} is expected to be nearly axially symmetric when a single conformer prevails and significantly asymmetric (or rhombic) when minor conformers, interconverting with the major conformer, are also populated. In the single-conformer scenario $|c_2^2| \approx 0$ and $|S_2^2| \approx 0$, whereas in the multiconformer scenario $|c_2^2| > 0$ and $|S_2^2| > 0$. In the latter case finer discrimination is based on the magnitude of $|c_2^2|$ or $|S_2^2|$. The *implicit* qualification of the contribution of side-chain rotamer jumps to ^{2}H spin relaxation through its effect on the symmetry and magnitude of the local coupling/ordering potential is physically sound and insightful. The SRLS approach can be extended to account *explicitly* for the flexibility of the methyl-bearing side chains. Recent studies by us[49−51] provide examples of how this might be accomplished.

Residual configurational entropy can be derived in the SRLS approach directly from P_{eq}, i.e., from experimentally determined c_0^2 and c_2^2 values. The MF strategy requires guessing the form of the potential after fitting, assuming it is axially symmetric, and using S^2, which is often inaccurate because of force-fitting.

II. Theoretical Background

A. The Model-Free Approach. The original MF approach considers an effective local motion decoupled from the (isotropic) global tumbling of the protein by virtue of the former being much faster than the latter.[19,20] On the basis of this premise the total time correlation function, $C(t)$, is factorized into the product of the time correlation for global motion, $C^C(t)$, and the time correlation function for local motion, $C^L(t)$

$$C(t) = C^C(t)C^L(t) \tag{1}$$

$C^C(t) = {}^1\!/_5 \exp(-t/\tau_m)$ for isotropic global motion, and $C^L(t)$ is taken as $C^L(t) = S^2 + (1 - S^2) \exp(-t/\tau_e)$.[19,20] The parameter $\tau_e \ll \tau_m$ denotes the effective local motion correlation time, and $C^L(\infty)$ is set equal to the square of a generalized order parameter, S^2.[19] The measurable spectral density, $J(\omega)$, is thus given by

$$J(\omega) = \frac{S^2\tau_m}{1 + \tau_m^2\omega^2} + \frac{(1 - S^2)\tau_e'}{1 + \tau_e'^2\omega^2} \tag{2}$$

where $1/\tau_e' = 1/\tau_m + 1/\tau_e \approx 1/\tau_e$. The ordering axis associated with the restricted local motion lies implicitly along the axial magnetic interaction. If several magnetic interactions are at play, then they are considered axial and collinear. Equation 2 was developed in early work as a perturbational expansion of the SRLS approach.[52]

When eq 2 cannot fit the experimental data, usually the extended MF spectral density[21]

$$J(\omega) = S_f^2\left[S_s^2\frac{\tau_m}{1 + \omega^2\tau_m^2} + (1 - S_s^2)\frac{\tau_s'}{1 + \omega^2 + \tau_s'^2}\right] +$$
$$(1 - S_f^2)\frac{\tau_f'}{1 + \omega^2\tau_f'^2} \tag{3}$$

is used. $1/\tau_f' \equiv 1/\tau_f + 1/\tau_m$ and $1/\tau_s' \equiv 1/\tau_s + 1/\tau_m$, where τ_s is the correlation time for slow local motion associated with a squared order parameter, S_s^2, and $\tau_f \ll \tau_s$ is the correlation time for fast local motion associated with a squared generalized order parameter, S_f^2. The local motions are mutually decoupled and independent of the global motion. Although the extended MF formula (eq 3) is based on eq 1, which requires that τ_m be much slower than both τ_s and τ_f, in practice it is applied to cases where the slow local motion (τ_s) occurs on the same time scale as the global tumbling (τ_m).

1. The MF Approach as Applied to ^{2}H Relaxation. Equation 2, which treats a single restricted local motion, has been adapted to methyl dynamics where two restricted local motions, occurring *around* and *of* the methyl averaging axis, are considered. The motion *around* the averaging axis has been associated with a squared order parameter $[P_2(\cos 110.5°)]^2 = 0.1$, and the motion *of* the averaging axis with S_{axis}^2.[24] S^2 was set equal to $0.1S_{axis}^2$, assuming that the two local motions are decoupled and that S_{axis}^2 is a squared *axial* order parameter.[24] The effective correlation time τ_e has been associated with *both* local motions. This yields the spectral density[11]

$$J(\omega) = \frac{S_{axis}^2 0.1\tau_m}{1 + \omega^2\tau_m^2} + \frac{(1 - S_{axis}^2 0.1)\tau_e'}{1 + \omega^2\tau_e'^2} \tag{4}$$

where $1/\tau_e' = 1/\tau_e + 1/\tau_m$. The fitting parameters are S_{axis}^2 and τ_e, with τ_m determined typically with ^{15}N spin relaxation.

A spectral density similar to eq 4, where τ_m is replaced with an effective correlation time, τ_{eff}, representing both the slow nanosecond local motions and the global tumbling, has been suggested.[13] τ_{eff} is allowed to vary in the fitting process. This formula yielded better fitting than eq 3 and enhanced versions thereof.[13,53]

2. The MF Approach as Applied to $\eta_{HC−HH}$ Cross-Correlation. Within a good approximation, only the dipolar ^{1}H−^{13}C and ^{1}H−^{1}H interactions need to be considered in the expression for $\eta_{HC−HH}$, and only $J(0)$ enters the calculation.[18] It is assumed that τ_e is so fast that only the global motion term of eq 4 persists. Its numerical coefficient is $P_2(\cos 110.5°)P_2(\cos 90°)$, where 90° represents the angle between the H−H direction and the methyl rotation axis.[18] This is the same as the result of two consecutive Wigner rotations from M to D and from D to D', where D and D' denote the H−C and H−H dipolar frames.

B. The Slowly Relaxing Local Structure Model. The fundamentals of the stochastic coupled rotator SRLS theory[42,43] as applied to biomolecular dynamics[44] have been outlined recently for NMR spin relaxation in proteins.[40,41,45−48] Two rotators, representing the global motion of the protein, R^C, and the effective local motion of the probe (C−D bond in this case), R^L, are treated. The motions of the protein and the probe are coupled by a local potential, $U(\Omega_{C'M})$, where C' denotes the local director fixed in the protein, and M denotes the local ordering/local diffusion frame fixed in the probe. In previous studies[40,42−48] we made use of a formalism involving Ω_{LM} and Ω_{LC}, where L denotes the fixed lab frame, and C the global diffusion frame. In a recent study,[41] we implemented a formalism involving $\Omega_{LC'}$, $\Omega_{C'M}$, and $\Omega_{CC'}$ (which are fixed Euler
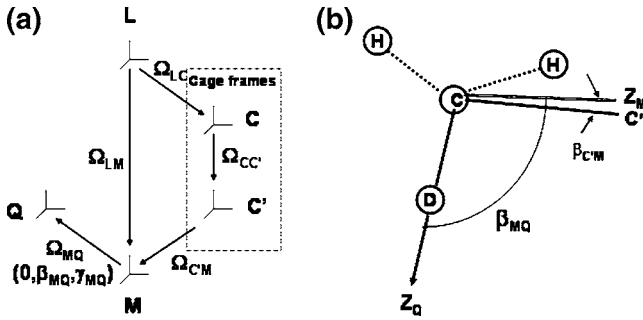
(a)

(b)

Figure 1. (a) Various reference frames that define the SRLS model: *L*, laboratory frame; *C*, global diffusion frame associated with protein shape; *C′*, local director frame fixed in the protein; *M*, local ordering/local diffusion frame fixed in the C−D bond; *Q*, quadrupolar tensor frame along the C−D bond. (b) Application to methyl dynamics. The simple case of motion about the rotation axis of the methyl group is illustrated. The equilibrium orientation of the C(methyl)−C bond (C$^\alpha$−C$^\beta$ for alanine, C$^\beta$−C$^{\gamma1}$ and C$^\beta$−C$^{\gamma2}$ for valine, etc.) is taken as the local director, *C′*. The local ordering frame, *M*, is assumed in this illustration for simplicity to be axially symmetric. Z_M orients preferentially parallel to *C′*. It also represents the methyl rotation axis, and it is tilted relative to Z_Q, i.e., the C−D bond, at $\beta_{MQ} = 110.5°$ (when $r_{CH} = r_{CD}$ is set equal to 1.115 Å, ref 17). The angle $\beta_{C'M}$ is the stochastic angle between the instantaneous orientation of the *M* frame, Z_M, and its equilibrium orientation, *C′*. For high ordering $\beta_{C'M}$ departs only slightly from zero.

angles; when the global motion is isotropic, the *C* and *C′* frames are the same and $\Omega_{CC'} = 0$). The relative orientation of the C−D bond in the protein, specified by the $\Omega_{C'M}$, is the more natural one in terms of conventional intuition. One can simply think of the Euler angles $\Omega_{C'M}$ as just being modulated by the local motion, whereas $\Omega_{LC'}$ is just modulated by the overall tumbling of the protein. Also, the $\Omega_{C'M}$ angles are the natural coordinates for expressing the potential energy. Of course, the two formalisms are mathematically equivalent.

The relative-coordinate formalism has been used in the present study. The various frames entering the SRLS model and the magnetic quadrupolar frame are shown in Figure 1. A brief summary of the formalism is given below.

Formally, the diffusion equation for the coupled system is given by

$$\frac{\partial}{\partial t} P(X,t) = -\hat{\Gamma} P(X,t) \quad (5)$$

where *X* is a set of coordinates completely describing the system

$$X = (\Omega_{C'M}, \Omega_{LC'})$$

$$\hat{\Gamma} = \hat{J}(\Omega_{C'M})\mathbf{R}^L P_{eq} \hat{J}(\Omega_{C'M}) P_{eq}^{-1} + [\hat{J}(\Omega_{C'M}) - \hat{J}(\Omega_{LC'})]\mathbf{R}^C P_{eq}[\hat{J}(\Omega_{C'M}) - \hat{J}(\Omega_{LC'})] P_{eq}^{-1} \quad (6)$$

where $\hat{J}(\Omega_{C'M})$ and $\hat{J}(\Omega_{LC'})$ are the angular momentum operators for the probe and the protein, respectively.

The Boltzmann distribution $P_{eq} = \exp[-u(\Omega_{C'M})]/\langle \exp[-u(\Omega_{C'M})]\rangle$ is defined with respect to the rescaled probe−cage interaction potential given by

$$u(\Omega_{C'M}) = \frac{U(\Omega_{C'M})}{k_B T} = -c_0^2 D_{0,0}^2(\Omega_{C'M}) - c_2^2[D_{0,2}^2(\Omega_{C'M}) + D_{0,-2}^2(\Omega_{C'M})] \quad (7)$$

This represents the expansion in the full basis set of the Wigner rotation matrix elements, $D_{KM}^L(\Omega_{C'M})$, with only lowest-order, i.e., $L = 2$, terms being preserved. The coefficient

c_0^2 (given in units of $k_B T$) is a measure of the orientational ordering of the C−D bond with respect to the local director, *C′*, whereas c_2^2 measures the asymmetry of the ordering around the director.

Time correlation functions are calculated as

$$C_{M,KK'}^J(t) = \langle D_{M,K}^J{}^*(\Omega_{LM})| \exp(-\hat{\Gamma}t)|D_{M,K'}^J(\Omega_{LM})P_{eq}\rangle \quad (8)$$

Their Fourier−Laplace transforms yield the spectral densities $j_{MKK'}^J(\omega)$, particular values of which determine the experimental relaxation rates.

In the case of zero potential, $c_0^2 = c_2^2 = 0$, the solution of the diffusion operator associated with the time evolution operator features three distinct eigenvalues

$$1/\tau_K = 6R_\perp^L + K^2(R_\|^L - R_\perp^L) \quad \text{for} \quad K = 0, 1, 2 \quad (9)$$

where $R_\|^L = 1/(6\tau_\|)$ and $R_\perp^L = 1/(6\tau_\perp) = 1/(6\tau_0)$. Only the diagonal terms, $j_{KK}(\omega)$ (the functions $j_{KK'}$ denote the real part of $j_{M,KK'}^2$; see ref 41), are nonzero, and they can be calculated analytically as Lorentzian spectral densities, each defined by width $1/\tau_K$. When the ordering potential is axially symmetric, $c_0^2 \neq 0$ and $c_2^2 = 0$, again only diagonal terms persist, but they are given by infinite sums of Lorentzian spectral densities that are defined in terms of eigenvalues $1/\tau_i$ of the diffusion operator and weighing factors $c_{K,i}$, such that

$$j_K(\omega) = \sum_i \frac{c_{K,i}\tau_i}{1 + \omega^2\tau_i^2} \quad (10)$$

The eigenvalues $1/\tau_i$ represent modes of motion of the system, in accordance with the parameter range considered. Note that although in principle the number of terms in eq 10 is infinite in practice a finite number of terms is sufficient for numerical convergence of the solution.

Finally, when the local ordering potential is rhombic, $c_0^2 \neq 0$ and $c_2^2 \neq 0$, both diagonal $j_K(\omega)$ and nondiagonal $j_{KK'}(\omega)$ terms are different from zero and need to be evaluated explicitly according to expressions analogous to eq 10.

The spectral densities $j_{KK'}(\omega)$ are defined in the *M* frame. If the *M* frame and the magnetic frame are tilted, then a Wigner rotation will be required to obtain the measurable autocorrelated spectral density, $J^{XX}(\omega)$ (*X* denotes the magnetic interaction), from the $j_K(\omega)$ and $j_{KK'}(\omega)$ spectral densities. Due the additional symmetry $j_{M,K,K'} = j_{M,-K,-K'}$, only the diagonal terms, $j_K(\omega)$, with $K = 0$, 1, and 2, and the nondiagonal terms, $j_{KK'}(\omega)$, with $KK' = (-2,2)$, $(-1,1)$, $(-1,2)$, $(0,1)$, $(0,2)$, and $(1,2)$ need to be considered.

For (axial) quadrupole autocorrelation, one has the explicit expression

$$J^{QQ}(\omega) = d_{00}^2(\beta_{MQ})^2 j_{00}(\omega) + 2d_{10}^2(\beta_{MQ})^2 j_{11}(\omega) + 2d_{20}^2(\beta_{MQ})^2 j_{22}(\omega) + 4d_{00}^2(\beta_{MQ})d_{20}^2(\beta_{MQ}) j_{02}(\omega) + 2d_{-10}^2(\beta_{MQ})d_{10}^2(\beta_{MQ})j_{-11}(\omega) + 2d_{-20}^2(\beta_{MQ})d_{20}^2(\beta_{MQ})j_{-22}(\omega) \quad (11)$$

with only the diagonal terms, $j_K(\omega)$, with $K = 0$, 1, and 2, and the nondiagonal terms, $j_{KK'}(\omega)$, with $KK' = (0,2)$, $(-1,1)$, and, $(-2,2)$ contributing.

A convenient measure of the orientational ordering of the C−D bond is provided by the order parameters, $S_0^2 = \langle D_{00}^2(\Omega_{C'M})\rangle$ and $S_2^2 = \langle D_{02}^2(\Omega_{C'M}) + D_{0-2}^2(\Omega_{C'M})\rangle$, which are

related to the orienting potential (eq 7), hence c_0^2 and c_2^2, via the ensemble averages

$$\langle D_{0n}^2(\Omega_{C'M})\rangle = \frac{\int d\Omega_{C'M}\, D_{0n}^2(\Omega_{C'M}) \exp[-u(\Omega_{C'M})]}{\int d\Omega_{C'M} \exp[-u(\Omega_{C'M})]} \quad (12)$$

One may convert to Cartesian ordering tensor components according to $S_{zz} = S_0^2$, $S_{xx} = (\sqrt{3/2}S_2^2 - S_0^2)/2$, and $S_{yy} = -(\sqrt{3/2}S_2^2 + S_0^2)/2$. Note that $S_{xx} + S_{yy} + S_{zz} = 0$.

For ^{2}H relaxation the measurable quantities are $J^{QQ}(0)$, $J^{QQ}(\omega_D)$, and $J^{QQ}(2\omega_D)$. Together with the squared magnetic quadrupole interaction they determine the experimentally measured relaxation rates according to standard expressions for NMR spin relaxation.[11] With C−D, H−H, and C−H fixed in the methyl group, the functions $j_K(\omega)$ and $j_{KK'}(\omega)$ associated with autocorrelated ^{2}H spin relaxation in ^{13}CH$_2$D also apply to cross-correlated HC−HH spin relaxation in ^{13}CH$_3$. All one has to do is to account properly for the local geometry and incorporate adequately the relevant magnetic interactions in assembling $J^{XY}(\omega)$ (X and Y denote the dipolar ^{13}C−^{1}H and ^{1}H−^{1}H interactions, respectively) out of the $j_K(\omega)$ and $j_{KK'}(\omega)$ functions.

In the present study we allowed for a maximum of four fitting parameters including c_0^2 and c_2^2 (potential coefficients), R^C/R^L, and β_{MQ}. We used $R^C = 1/6\tau_m$ with τ_m as determined in refs 13 and 18 based on ^{15}N T_1/T_2 ratios.[54] For axial local potentials the SRLS spectral density is formally (but not physically) analogous to the reduced extended MF formula (where the third term of eq 3 is set equal to zero). For rhombic potentials the SRLS approach features one extra parameter, c_2^2. When the potential is axially symmetric and β_{MQ} is set equal to zero, then the SRLS spectral density is formally analogous to the original MF spectral density.

The functions $j_K(\omega)$ (eq 10) and $j_{KK'}(\omega)$ (equations analogous to eq 10) are calculated on the fly. In the methyl dynamics application the local potentials are (due to fast methyl rotation about a "diffusion tilt" of 110.5°) relatively low, with $|c_0^2|$ and $|c_2^2|$ on the order of 1−2 (in units of $k_B T$). The time scale separation of $R^C/R^L \approx 0.02$, determined with data fitting (see below), is also not too large. The computational effort was found to be very reasonable in this case. Thus, it took 10−40 min on a 3.2 GHz Pentium 4 processor to fit two-field ^{2}H T_1 and T_2 data sets of a given methyl group of protein L. Our SRLS-based fitting program is similar to the MF fitting programs. The only extra requirement on the part of the user is to determine a truncation parameter that controls the number of terms that need to be taken into account for convergence of the solution (given by eq 10 or similar equations). Several trial and error calculations carried out for typical cases suffice. Our current software is available upon request. The "Theoretical Background" section of ref 41 contains all the information needed for ab initio programming.

The MF results for protein L were taken from the papers of Kay et al.,[13,18] and the MF results for ubiquitin from ref 8.

C. A Survey of SRLS and MF Analysis of Methyl Dynamics. Oversimplified theoretical spectral densities lead to force fitting because the best-fit parameters absorb the differences from the exact experimental spectral density. Reasons for this in methyl dynamics are outlined below.

Equation 2 constitutes an approximation to the exact SRLS solution in the limit where the time scale separation between the global and the local motions is large, i.e., $R^C/R^L \ll 1$, and the axial local ordering is either very small (perturbation limit)[52]

or very high (Born−Oppenheimer (BO) limit).[55] The validity of these assumptions cannot be tested within the scope of the MF approach. Since the SRLS approach allows for arbitrary R^C/R^L and arbitrary local ordering and given that the SRLS approach yields the MF approach in appropriate asymptotic limits,[40] one can determine by comparison whether eq 2 is valid. In the BO limit S^2 represents $(S_0^2)^2$ and τ_e represents the renormalized local motion correlation time, $\tau_{ren} \approx 2\tau_0/c_0^2$. The quantities S_0^2 and τ_{ren} are well-defined physical parameters. We examined previously the BO limit, which applies to backbone ^{15}N spin relaxation, to find frequent digressions, with S^2 and τ_e representing in these cases inaccurate force-fitted parameters.[40,41,45−48] In this study we examine the perturbation limit, which applies to methyl ^{2}H spin relaxation, wherein S^2 represents $(S_0^2)^2$ and τ_e represents τ_0. Note that eq 3 is also a perturbational expansion of the SRLS approach for rhombic ordering in the $R^C/R^L \ll 1$ limit,[56] typically used outside of its validity range.[40,41,45−48]

Equation 4 is the same as eq 2 with S^2 recast as $0.1S_{axis}^2$. The form of eq 2 corresponds to $j_K(\omega)$ with $K = 0$.[40,52] Equation 2 represents the measurable spectral density, $J^{QQ}(\omega)$; hence $J^{QQ}(\omega) = j_0(\omega)$. This is only valid when the local diffusion frame, M, and the magnetic frame, Q, are collinear, which is not the case for $\beta_{MQ} = 110.5°$. For a tilted axial M frame the functions $j_1(\omega)$ and $j_2(\omega)$ should also be included in the expression for $J^{QQ}(\omega)$. The weighting factors of $j_0(\omega)$, $j_1(\omega)$, and $j_2(\omega)$ for $\beta_{MQ} = 110.5°$ are $(d_{00}^2)^2 = 0.1$, $2(d_{10}^2)^2 = 0.323$, and $2(d_{20}^2)^2 = 0.577$ (where d_{MK}^2 denote the reduced Wigner matrix elements of rank 2). The magnitudes of the $K = 1$ and $K = 2$ contributions to $J^{QQ}(\omega)$ for typical values of S^2 and τ_e are 10% and 20%, respectively. The MF approach does not feature $j_1(\omega)$ and $j_2(\omega)$. Ignoring the $K = 1$ and $K = 2$ contributions is only valid in the limit where the local motion is so fast that it enters the analysis only through its effect on the squared order parameter, S^2, i.e., in the limit where the second term of eqs 2 and 4 is zero.

A further issue to consider is the interpretation of S_{axis}^2 as amplitude of motion. This interpretation is appropriate when the local motion is in the extreme motional narrowing limit ($\tau_e \rightarrow 0$), where S^2 represents the mean-squared fluctuation amplitude of all the internal motions, and may eventually be expressed as $0.1S_{axis}^2$.

Equation 2 corresponds to axial local ordering. In this case the local ordering tensor features a single nonzero principal value, $S_0^2 = \langle P_2(\cos \beta_{C'M})\rangle$. For rhombic symmetry the local ordering tensor features two nonzero principal values, S_0^2 and S_2^2. The sensitivity of backbone ^{15}N relaxation rates to the rhombic symmetry of the local ordering was demonstrated with the three-dimensional (3D) Gaussian axial fluctuations (GAF) model, which is applicable when the local motions are very fast,[57] and with the SRLS approach, which is applicable in general.[40,41] We show herein that side-chain ^{2}H relaxation rates are also sensitive to the asymmetry of the local ordering. As pointed out above, for rhombic local ordering nondiagonal functions $j_{KK'}(\omega)$ also contribute to $J^{QQ}(\omega)$.

Rhombic ordering is particularly important in the context of side-chain dynamics. As pointed out above, the potential coefficients, c_0^2 and c_2^2, and the order parameters, S_0^2 and S_2^2 (defined in terms of c_0^2 and c_2^2 using $P_{eq} = -\exp(u)$), discriminate between single-rotamer scenarios, where $|c_2^2| \approx 0$ and $|S_2^2| \approx 0$, and multiple rapidly interconverting rotamer scenarios, where $|c_2^2| > 0$ and $|S_2^2| > 0$.

P_{eq} can be used to calculate residual configurational entropy or any other thermodynamic quantity. The form of the potential,

20620 *J. Phys. Chem. B, Vol. 110, No. 41, 2006*

Meirovitch et al.

TABLE 1: Best-Fit Parameters Obtained with SRLS Fitting of the Experimental ^2H T_1 and T_2 Methyl Relaxation Rates of Protein L[a]

	SRLS		MF		
	c_0^2	τ^L, ps (τ^L/τ_m)	$c_0^2(MF)^b$	τ_e, ps (τ_e/τ_m)	S_{axis}^2
		High S_{axis}^2 Value			
T3	0.92	13 (0.003)	1.32	39 (0.010)	0.88
I4γ	0.89	8.9 (0.002)	1.32	24 (0.006)	0.87
A6	0.88	23.9 (0.006)	1.27	71 (0.017)	0.80
I9g	0.86	9.7 (0.002)	1.25	29 (0.007)	0.77
A11	0.91	13.4 (0.003)	1.36	49 (0.012)	0.82
A18	0.87	19.8 (0.005)	1.28	57 (0.014)	0.81
T23	0.89	14.2 (0.004)	1.30	39 (0.010)	0.84
A27	0.92	27.9 (0.007)	1.32	85 (0.021)	0.86
T28	0.94	13.8 (0.003)	1.32	41 (0.010)	0.88
A31	0.88	26.7 (0.007)	1.30	77 (0.019)	0.83
A35	0.90	43.3 (0.010)	1.27	133 (0.033)	0.80
A50	0.89	7.3 (0.002)	1.30	24 (0.006)	0.84
T55	0.96	19.4 (0.005)	1.40	51 (0.013)	0.98
I58γ	0.88	8.1 (0.002)	1.29	27 (0.007)	0.82
V2γ_1	0.84	17.8 (0.004)	1.22	54 (0.013)	0.73
T37	0.86	16.6 (0.004)	1.23	50 (0.012)	0.74
		Medium/Low S_{axis}^2 Value			
T15	−0.88	24.3 (0.006)	1.08	69 (0.017)	0.57
T46	−1.04	21.9 (0.005)	1.18	63 (0.016)	0.69
L38δ_1	−0.90	11.7 (0.003)	1.07	34 (0.008)	0.56
L38δ_2	−0.85	14.2 (0.004)	0.98	42 (0.010)	0.47
V47γ_1	−0.97	18.2 (0.004)	1.08	55 (0.014)	0.57
V47γ_2	−1.03	27.9 (0.007)	1.16	78 (0.019)	0.66
V49γ_1	+0.81	11.7 (0.003)	1.17	34 (0.008)	0.68
V49γ_2	−1.01	12.6 (0.003)	1.13	40 (0.010)	0.62
L56δ_1	−0.96	25.5 (0.006)	1.12	70 (0.017)	0.61
L56δ_2	+0.78	12.6 (0.003)	1.12	38 (0.009)	0.61
I58γ	−0.95	5.3 (0.001)	1.09	17 (0.004)	0.58
A61	−0.99	15.0 (0.004)	1.11	46 (0.011)	0.60
I9δ	−0.77	6.5 (0.002)	0.92	24 (0.006)	0.38
	Methyl Groups that Required Special Treatment in the MF Analysis^c				
I4δ	−0.70	11.7 (0.003)			
L8δ_1	−0.43	19.0 (0.005)			
L8δ_2	−0.58	17.0 (0.004)			
T17	−0.94	26.7 (0.007)			

^{a} $\tau_m = 4.05$ ns was used.[13] The variables in the fitting process were c_0^2 and τ^L/τ_m. The results of the MF analysis of Srynnikov et al.[13] are given as $c_0^2(MF)$ derived from S^2 using eqs 7 and 12 and τ_e/τ_m. The values of τ^L, τ_e, and $S_{axis}^2 = S^2/0.1$ are also shown. Excluding the methyl groups I4δ, L8δ_1, L8δ_2, and T17, which could not be fit in the MF approach with model 2, χ^2 is typically below 2 in the SRLS calculations. The data shown are grouped according to the values of S_{axis}^2; the methyl groups I4δ, L8δ_1, L8δ_2, and T17 are presented at the bottom of the table. ^{b} Note that $c_0^2 = 1.42$ corresponds to $S_{axis}^2 = 1$. ^{c} The χ^2 values for these residues are $\chi^2 = 9$ for I4δ, $\chi^2 = 14$ for L8δ_1, $\chi^2 = 30$ for L8δ_2, and $\chi^2 = 4$ for T17.

u, is as general as warranted by the experimental data. The coefficients c_0^2 and c_2^2 are determined with data fitting. These are new features of analysis. In the MF approach the form of the potential has to be guessed after fitting, its symmetry must be axial (see definition of S_{axis}^2 in ref 24), and the accuracy of the calculated residual configurational entropy depends on the accuracy of S^2, which is shown herein to be problematic.

III. Results and Discussion

A. Protein L.[12,13,18,31] SRLS-based fitting of the ^2H methyl relaxation data of Millet et al.[12] acquired at 11.7 and 14.1 T and 25° C was carried out. Table 1 shows the best-fit SRLS parameters obtained with a model where the protein exerts an axial potential $u = -c_0^2 P_2(\cos \beta_{C'M})$ at the site of the motion of the methyl group. The latter experiences (fast) local motion approximated as isotropic, with correlation time $\tau^L = \tau_0 = 1/6R^L$.

TABLE 2: Eigenvalues, $1/\tau_i$, and Weighting Factors, $c_{K,i}$, of the SRLS Solution for $C_0(t)$, $C_1(t)$, and $C_2(t)$ Obtained Using $c_0^2 = 1.3$ and $R^C/R^L = 0.01^a$

SRLS			MF	
$C_0(t)$			$C_0(t)$	
$1/\tau_i$	$c_{K,i}$	$(d_{00}^2)^2$	$1/\tau_i$	$c_{K,i}$
5.69	0.340	0.100	6	0.916
6.16	0.337			
7.49	0.222			
19.67	0.012			
20.40	0.0023			
0.06	0.085		0.06	0.084

$C_1(t)$		
$1/\tau_i$	$c_{K,i}$	$2(d_{10}^2)^2$
6.15	0.328	0.323
6.56	0.273	
6.91	0.244	
1.61	0.140	
19.84	0.010	
20.16	0.002	

$C_2(t)$		
$1/\tau_i$	$c_{K,i}$	$2(d_{20}^2)^2$
5.09	0.584	0.577
6.96	0.336	
7.59	0.073	
20.31	0.005	

^{a} The coefficients $(d_{00}^2)^2$, $2(d_{10}^2)^2$, and $2(d_{20}^2)^2$ correspond to $\beta_{MQ} = 110.5°$. The best-fit MF parameters obtained[13] for methyl T23, $S^2 = 0.084$, correspond to $c_0^2 = 1.3$ (eqs 7 and 12 with $c_2^2 = 0$) and $\tau_e/\tau_m = 0.01$.

The parameters varied in the fitting process were c_0^2 and τ^L/τ_m, and the order parameter S_0^2 was calculated in terms of the potential, U. The principal axis of the axial ordering tensor was taken to lie along the C−D bond, i.e., $\beta_{MQ} = 0$.

This SRLS variant used is formally analogous to the original MF formula (eq 2) used in MF model 2. The SRLS spectral density is given by c_0^2 and τ^L, whereas the MF spectral density is given by $S^2 = 0.1S_{axis}^2$ and τ_e. As indicated above, when mode coupling can be neglected so that eq 2 constitutes a good approximation of eq 10, S^2 is an approximation to $(S_0^2)^2$. Hence, the potential in terms of which S_0^2 is defined can be associated with S^2. We calculated $c_0^2(MF)$ from S^2 (taken from ref 13) according to eqs 7 and 12 and compared it with $c_0^2(SRLS)$. $\tau^L = 1/6R^L$ was compared with τ_e. These data are presented in Table 1 together with S_{axis}^2 (taken from ref 13). If significant differences between the corresponding SRLS and MF parameters are observed, then this will indicate that mode coupling cannot be ignored.

We compare potential coefficients since they are the generic physical quantities that enter the stochastic SRLS model of which the MF approach is a limiting case. Squared order parameters determine the weighting factors of the global and local motion modes only in the BO[55] or perturbation[52,56] limits.

Let us illustrate the effect of mode coupling, which renders the SRLS results in Table 1 different from their MF counterparts. We selected methyl T23, for which MF analysis yielded the best-fit parameters of $\tau_e/\tau_m = 0.01$ and $S^2 = 0.84$, as a representative example. These quantities (with $S^2 = 0.84$ "translated" into $c_0^2 = 1.3$ using eqs 7 and 12) were used as input to an SRLS calculation. The latter yielded the eigenvalues, $1/\tau_i$, and weighting factors, $c_{K,i}$, shown in Table 2 (See eq 10

SRLS/NMR Analysis of Methyl Dynamics in Proteins

J. Phys. Chem. B, Vol. 110, No. 41, 2006 **20621**

for the definitions of τ_i and $c_{K,i}$.) The MF results, with the bare local motion eigenmode equal to 6, the bare global motion eigenmode equal to 0.01 (in units of R^L), and the corresponding weighting factors equal to 0.916 and 0.084, respectively, are also shown. The (asymptotic) MF time correlation function is $C_{K=0}(t)$.

The $C_0(t)$ SRLS time correlation function comprises three local motion eigenmodes with eigenvalues near to, but not equal to, 6, with a combined fractional contribution of 0.899. Two fast mixed eigenmodes make a fractional contribution 0.0143, and the global motion eigenmode, with $1/\tau = 0.06$, contributes 0.085. The eigenmodes shown constitute 0.998 of $C_0(t)$, with the remaining 0.002 fraction contributed by a large number of eigenmodes with very small individual weights.

The $C_1(t)$ time correlation function is made of three local motion eigenmodes with eigenvalues close to 6, which together make a fractional contribution of 0.845. There is a mixed mode with an eigenvalue 1.61 and a fractional contribution of 0.14, and two fast mixed modes with a combined contribution of 0.012. The eigenmodes shown constitute 0.997 of $C_1(t)$, with the remaining 0.003 fraction contributed by a large number of eigenmodes with very small individual weights. The $C_2(t)$ time correlation function comprises three local motion modes with eigenvalues that differ quite a bit from 6. Their combined fractional contribution is 0.993. A fast eigemmode contributes 0.0053. The eigenmodes shown constitute 0.9983 of $C_2(t)$, with the remaining 0.0017 fraction contributed by a large number of eigenmodes with very small individual weights.

The "diffusion tilt" for methyl rotation is $\beta_{MQ} = 110.5°$. For this tilt angle the fractional contribution of the $C_K(t)$ functions to $C(t)$ and of the $j_K(\omega)$ functions to $J^{QQ}(\omega)$ is $(d_{00}^2)^2 = 0.1$, $2(d_{10}^2)^2 = 0.323$, and $2(d_{20}^2)^2 = 0.577$ for $K = 0, 1$, and 2, respectively. The value of β_{MQ} is implicitly zero in the original MF formula used to obtain the MF results shown in Table 1. To enable comparison with the MF approach, the angle β_{MQ} was set deliberately equal to zero in the SRLS calculations of Table 1. $\beta_{MQ} = 0$ implies $(d_{00}^2)^2 = 1$ and $2(d_{10}^2)^2 = 2(d_{20}^2)^2 = 0$; hence $J^{QQ}(\omega) = j_0(\omega)$. Obviously, this constitutes an oversimplification. The postfitting decomposition of S^2 into $0.1 S_{axis}^2$ is not the same as carrying out rigorously the frame transformation from M to Q whereby $J^{QQ}(\omega)$ is properly assembled out of the (multimode) $j_K(\omega)$ functions. The MF strategy is only appropriate in the limit where the $j_K(\omega)$ functions are given solely by the global motion mode.

Clearly $C_0(t)$(SRLS) differs from $C_0(t)$(MF), implying the different results shown in Table 1.

The methyl groups in Table 1 have been classified according to the magnitude of S_{axis}^2, which was determined in ref 13. For methyl groups associated with high S_{axis}^2, we found that c_0^2(SRLS) is on the order of 0.9 whereas c_0^2(MF) is on the order of 1.32, i.e., higher by 47%. Clearly the actual strength of the spatial restrictions is *overestimated* by the MF approach in the parameter range corresponding to high S_{axis}^2. The methyl groups associated with medium/low S_{axis}^2 yield negative c_0^2 values. Since the diffusion tilt was fixed at 0° in the SRLS calculations, the fact that c_0^2 is negative indicates that the experimental data are sensitive to the 110.5° diffusion tilt. The equilibrium value (minimum) of $u = -c_0^2 P_2(\cos \beta_{C'M})$ occurs for $\beta_{C'M} = \beta_{MQ}$. Since $P_2(\cos \beta_{C'M}) < 0$ for $\beta_{C'M} = \beta_{MQ} = 110.5°$, one must have $c_0^2 < 0$ for u to be negative at its equilibrium position. The minimum of u for $c_0^2 < 0$ is only half as deep as the minimum for $c_0^2 > 0$. Since the MF approach fits S^2, squared order parameters need to be considered. Calculations

TABLE 3: MF and SRLS Calculations of η_{HC-HH} of Residue V49γ_1[a]

	c_0^2	S_{axis}^2	τ^L/τ_m	β_{MQ}	η_{HC-HH}, s^{-1}
MF	1.18	0.68	0.007	0° implicit	24.9
MF	1.2	0.70	0.0	0° implicit	23.6
SRLS		1.2	0.001 (0)	0° fixed	23.5

[a] The axial potential $u = -c_0^2 P_2(\cos \beta_{C'M})$ was used to derive c_0^2(MF) from $S^2 = 0.1 \times 0.68$ in row 1 and from $S^2 = 0.1 \times 0.70$ in row 2, using eqs 7 and 12. The values of $\theta = 110.5°$ and $r_{CD} = 1.115$ Å were used. The global motion correlation time employed was $\tau_m = 5$ ns (D$_2$O solution). The experimental value of η_{HC-HH} is 23.6 s^{-1}.[18] The χ^2 values were below 2 in the SRLS calculations.

showed that the squared order parameter corresponding to $c_0^2 \approx 1.0$ is approximately 1.7 times larger than the squared order parameter corresponding to $c_0^2 \approx -1.0$. For low ordering $(S_0^2)^2$ is within a good approximation in direct proportion to c_0^2.[45] Hence the negative SRLS c_0^2 values in Table 1 are to be multiplied by 1.7 when compared to the positive MF c_0^2 values. Thus, the MF approach *underestimates* the strength of the spatial restrictions in the parameter range corresponding to medium/low S_{axis}^2 values. This is yet another illustration of the fact that force fitting depends on the parameter range. The local motion correlation time, τ^L, is on average overestimated by τ_e. Clearly the MF picture is different from the SRLS picture. It can be seen that the distribution in S_{axis}^2, which is the main qualifier of methyl dynamics, extends to values that are too high and too low.

The methyl groups I4δ, T15, L8δ_1, and L8δ_2 could not be fit in the MF approach with eq 2. A modified version of the extended MF formula had to be used to analyze the data of these methyl groups.[13,53] Except perhaps for L8δ_2, which yielded $\chi^2 = 30$ in the SRLS analysis, these methyl groups may be included in the low/medium S_{axis}^2 category with a somewhat lenient χ^2 threshold.

We consider now the η_{HC-HH} cross-correlated relaxation rate. Relevant calculations, all associated with low χ^2 values, are shown in Table 3. The methyl group V49γ_1 was selected as a representative example. The experimental value measured for this methyl group at 25° is 23.7 s^{-1}.[18] When the best-fit MF value of $S_{axis}^2 = 0.68$, derived with ^{2}H analysis, is used to calculate η_{HC-HH} according to eq 2 of ref 18, one obtains $\eta_{HC-HH} = 24.9$ s^{-1} (row 1). When S_{axis}^2 is derived from eq 2 of ref 18, one obtains $S_{axis}^2 = 0.7$ (row 2). Practically the same S_{axis}^2 is obtained with ^{2}H autocorrelation and η_{HC-HH} cross-correlation, however, with spectral densities which feature *different* parameter combinations. Thus, $J(0)$ used to analyze η_{HC-HH} has τ_e set equal to zero, whereas $J(\omega)$ used to fit the ^{2}H data features finite τ_e values that affect the analysis significantly.

The fact that at 25 °C similar S_{axis}^2 values can be obtained with $\tau_e \neq 0$ for ^{2}H relaxation analysis and $\tau_e = 0$ for η_{HC-HH} analysis appears to be related to the fact that in the MF parametrization scenario the quantity ^{2}H $1/T_2$, given mainly by $J(0)$, and the quantity η_{HC-HH}, given by $J(0)$, depend predominantly on S_{axis}^2. However, the quantity ^{2}H $1/T_1$, given by $J(\omega)$ and $J(2\omega)$, depends predominantly on τ_e. This was pointed out earlier by Ishima et al.[16] for ^{13}C T_1 and T_2 in the context of ^{13}CD$_2$H relaxation.

At this stage we tried to reproduce η_{HC-HH} based on the results of the ^{2}H analysis. We found that the combination of best-fit SRLS parameters obtained from the ^{2}H relaxation analysis of V49γ_1 (Table 1) does not reproduce properly the experimental η_{HC-HH} value. The latter can be reproduced in the SRLS approach with the same scenario as in the MF approach,

20622 *J. Phys. Chem. B, Vol. 110, No. 41, 2006*

Meirovitch et al.

TABLE 4: SRLS Calculation of η_{HC-HH} as Described in Detail in the Text[a]

c_0^2	τ^L/τ_m	β_{MQ}	$R_\parallel^L/R_\perp^L$	η_{HC-HH}, s^{-1}
1	2	3	4	5
1 0.81	0.003	fixed at 0°	fixed at 1	~11.3
2 0.86	0.003	22.0°	fixed at 1	~8.3
3 2.5	0.055	fixed at 0°, $Q(^2H) \times 0.1$	fixed at 1	~113.3
4 2.7	0.002	fixed at 110.5°	fixed at 1	~36.1
5 1.81	0.008	37.6°	15.1	~40.0

[a] The axial potential $u = -c_0^2 P_2(\cos \beta_{CM})$ was used. The global motion correlation times were $\tau_m = 4.05$ ns for ^{2}H relaxation[13] (columns 1–4) and 5 ns for η_{HC-HH} relaxation[18] (column 5). τ^L/τ_m denotes the time scale separation between the global and the local motions, β_{MQ} the "diffusion tilt", and $R_\parallel^L/R_\perp^L$ the anisotropy of the local diffusion tensor. $Q(^2H)$ represents the coefficient of $J^{QQ}(0)$ in the expression of η_{HC-HH}, including the squared quadrupole interaction.

i.e., by setting τ^L practically equal to zero, as shown in row 3 of Table 3. This result is unacceptable. One needs to identify the SRLS variant that reproduces *both* ^{2}H relaxation and η_{HC-HH} cross-correlation. The particular parameter combination featured by this variant is likely to represent a physically appropriate model for methyl dynamics.

SRLS calculations carried out in this context, using the methyl group V49γ_1 as a representative example, are shown in Table 4. The parameters shown in columns 1–4 are best-fit values obtained with ^{2}H analyses featuring various parameter combinations. They constitute input values for the calculation of η_{HC-HH}, which is shown in column 5. $\tau_m = 4.05$ ns (H$_2$O solution) was used in the ^{2}H analyses, and $\tau_m = 5$ ns (D$_2$O solution) was used to calculate η_{HC-HH}. χ^2 was on the order of 2 in all the ^{2}H analyses.

The ^{2}H data in row 1 were taken from the Table 1 entry for V49γ_1. The parameters varied in the ^{2}H analysis include c_0^2 and τ^L/τ_m. Their best-fit values (columns 1–4) do not reproduce the experimental value of η_{HC-HH} (column 5). The ^{2}H data in row 2 are best-fit values obtained by varying c_0^2, τ^L/τ_m, and β_{MQ} (columns 1–4). These results do not differ significantly from those shown in row 1, except that $\beta_{MQ} = 22°$. η_{HC-HH} is not reproduced (column 5). The next model presented in row 3 is one where the motion *around* the "axis" is considered infinitely fast; hence $[P_2(\cos 110.5°)]^2 = 0.1$ was taken to scale the squared quadrupole interaction. c_0^2 and τ^L describe an effective local motion, excluding methyl rotation. This model is rejected for two reasons. First, if the motion *around* the "axis" is infinitely fast, then the local potential can only be equal to or smaller than 1.42, which corresponds to $S^2 = 0.1$. The value of 2.5 exceeds this limit. Second, η_{HC-HH} is not reproduced (column 5). In yet another attempt shown in row 4, the angle β_{MQ} was fixed at 110.5°, with c_0^2 and τ^L describing an effective local motion. This model is rejected for the same reasons as the model of row 3. In the last model presented in row 5, the parameters c_0^2, τ^L/τ_m, β_{MQ}, and $R_\parallel^L/R_\perp^L$ were allowed to vary in the ^{2}H analysis. This is formally analogous to the so-called "model 6" in the MF approach. This model represents the extension of the model presented in row 2 from isotropic to axial local diffusion. It is rejected for the same reasons that led to the rejection of the models presented in rows 2 and 3.

Clearly none of the SRLS models considered in Table 4 is satisfactory. The negative c_0^2 values in Table 1 are an indication that the symmetry of the local potential/local ordering is an important component of the model. We therefore proceed by allowing for rhombic potentials. For axial potentials, only the diagonal functions $j_K(\omega)$, $K = 0, 1$, and 2 (eq 10) are relevant, and the measurable spectral density, $J^{QQ}(\omega)$, is given

by linear combinations of these functions according to the local geometry. When the potential is rhombic, the spectral density $J^{QQ}(\omega)$ is given by a linear combination of $j_0(\omega)$, $j_1(\omega)$, $j_2(\omega)$, $j_{02}(\omega) = j_{20}(\omega)$, $j_{2-2}(\omega) = j_{-22}(\omega)$, and $j_{1-1}(\omega) = j_{-11}(\omega)$, according to the local geometry. To illustrate the effect of potential symmetry, we consider the case of $\tau^L/\tau_m = 0.001$. For such high time scale separation and axial potentials, one has $j_1(\omega), j_2(\omega) \ll j_0(\omega)$; hence $J^{QQ}(\omega) \cong j_0(\omega)$, implying that $\beta_{MQ} \cong 0$ (the coefficient of $j_0(\omega)$ in the expression for $J^{QQ}(\omega)$ is $(d_{00}^2)^2 = (1.5 \cos^2 \beta_{MQ} - 0.5)^2$). The functions $j_K(\omega)$ are illustrated in Figure 2a for $\tau^L/\tau_m = 0.001$ and $c_0^2 = 1.5$. The $j_K(\omega)$ and $j_{KK'}(\omega)$ functions calculated for a rhombic potential given by $c_0^2 = 2.0$ and $c_2^2 = 3$ and for $\tau^L/\tau_m = 0.001$ are shown in Figure 2b. $J^{QQ}(\omega)$ is given by a linear combination of these functions with coefficients determined by the value of β_{MQ}, which cannot be zero since the D frame is axial whereas the M frame is rhombic. For example, when $\beta_{MQ} \approx 90°$ only the functions $j_0(\omega)$, $j_2(\omega)$, and $j_{2-2}(\omega) = j_{-22}(\omega)$ contribute significantly. Clearly the symmetry of the potential as well as the local geometry affect profoundly the measurable spectral density, $J^{QQ}(\omega)$.

To further illustrate the large effect of the potential symmetry on the analysis, we calculated the components of the Cartesian ordering tensors corresponding to the potential coefficients of Figures 2a and 2b. Irreducible ordering tensor components, S_0^2 and S_2^2, were calculated from c_0^2 and c_2^2 according to eqs 7 and 12. S_{xx}, S_{yy}, and S_{zz} were then calculated from S_0^2 and S_2^2 as outlined after eq 12. For the rhombic potential given by $c_0^2 = 2$ and $c_2^2 = 3$, we obtained $S_{xx} = +0.306$, $S_{yy} = -0.394$, and $S_{zz} = +0.088$. The sign of a given Cartesian tensor component indicates whether the respective axis tends to align parallel to the local director (positive component) or perpendicular to it (negative component). The component with the largest absolute value corresponds to the main ordering axis, which in this case is Y_M, yielding so-called "Y_M ordering". The negative value of X_M is approximately equal to the positive value of Y_M. This yields what we call "nearly planar Y_M-X_M ordering/symmetry", with the first axis in this notation representing the main ordering axis. Similar scenarios will be denoted in an analogous fashion. Comparison with $S_{xx} = S_{yy} = -0.22$ and $S_{zz} = +0.44$, obtained for an axial potential of comparable strength given by $c_0^2 = 1.5$ points out the significant difference between axial ordering and nearly planar (rhombic) Y_M-X_M ordering. As shown below, nearly planar Y_M-X_M ordering is characteristic of methyl sites in proteins associated with low S_{axis}^2 values. The physical meaning of this and other symmetries of the local ordering associated with methyl dynamics are discussed below.

The sensitivity of the ^{2}H relaxation rates to the symmetry of the local potential is further illustrated in Figure 3, where we show ^{2}H T_1 and T_2 calculated for rhombic potentials given by $c_0^2 = 1$, c_2^2 varied from -0.5 to 2.0, $\beta_{MQ} = 22°$, $\tau^L/\tau_m = 0.017$, and $\tau_m = 3.5$ ns. The values of $c_0^2 = 1$ and $c_2^2 = -0.5$ correspond to Z_M ordering and relatively small rhombicity. The values of $c_0^2 = 1$ and $c_2^2 \approx 1.5$ correspond to nearly planar Y_M-X_M ordering. The values of $c_0^2 = 1$ and $c_2^2 \approx 1.75$ correspond to nearly planar X_M-Y_M ordering. The parameter sets used as input are typical of the SRLS results obtained for ubiquitin data[8] acquired at 30° C (see below). Practically the entire range of the experimental ^{2}H $1/T_1$ and $1/T_2$ values[8] is spanned by the ordinates of the panels of Figure 3.

On the basis of the substantial sensitivity of the analysis to potential rhombicity borne out by the calculations presented above and the various inconsistency-related problems encoun-
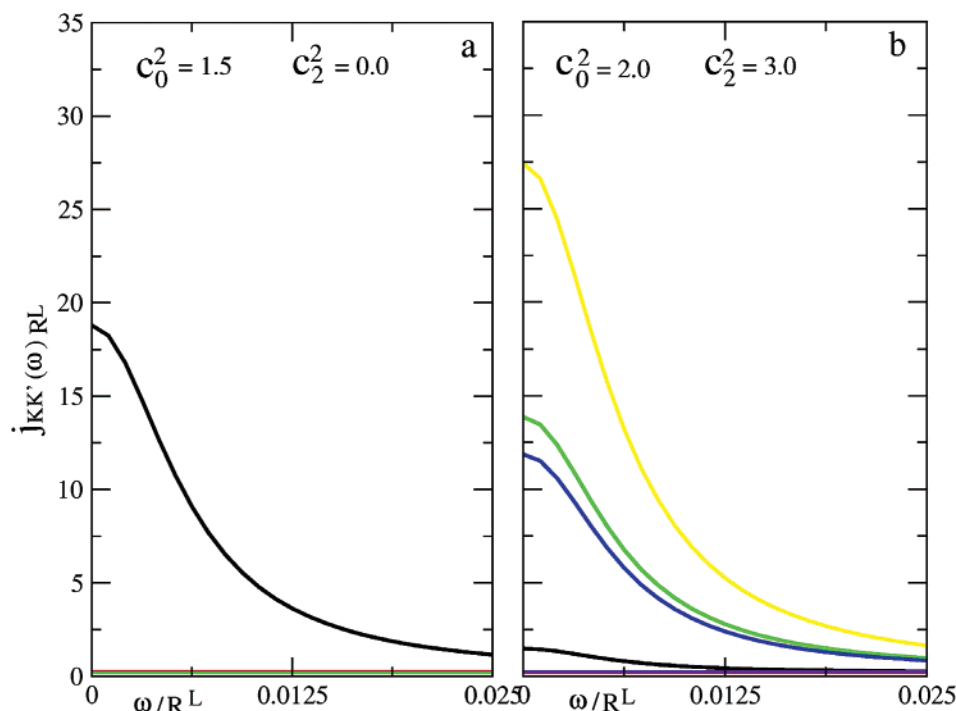
SRLS/NMR Analysis of Methyl Dynamics in Proteins

J. Phys. Chem. B, Vol. 110, No. 41, 2006 **20623**

Figure 2. (a) Spectral densities $j_{KK'}(\omega)$ in units of $1/R^L$ calculated for an axial potential with $c_0^2 = 1.5$ and $\tau^L/\tau_m = 0.001$. ($j_{KK'}(\omega)$ represents in this case $j_K(\omega)$, which is a shorthand notation for $j_{KK'}(\omega)$.) (b) Spectral densities $j_{KK'}(\omega)$ in units of $1/R^L$ calculated for a rhombic potential with $c_0^2 = 2.0$ and $c_2^2 = 3.0$ and $\tau^L/\tau_m = 0.001$. ($j_{KK'}(\omega)$ stands for both $j_K(\omega)$ and $j_{KK'}(\omega)$.) The abscissa, ω, is given in units of R^L. The black, red, and green curves represent the functions $j_0(\omega)$, $j_1(\omega)$, and $j_2(\omega)$, respectively. The blue, yellow, and indigo curves represent the functions $j_{20}(\omega) = j_{02}(\omega)$, $j_{2-2}(\omega) = j_{-22}(\omega)$, and $j_{1-1}(\omega) = j_{-11}(\omega)$, respectively.
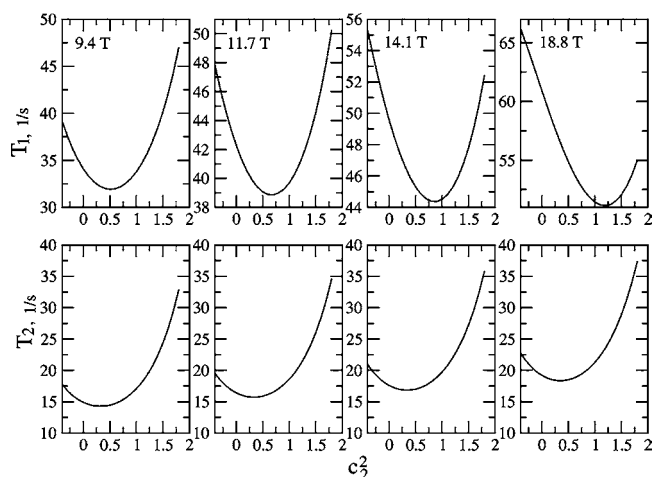

Figure 3. $1/T_1$ and $1/T_2$ ^{2}H relaxation rates calculated for $\tau^L/\tau_m = 0.017$, $\beta_{MQ} = 22°$, $c_0^2 = 1$, $\tau_m = 3.5$ ns, and c_2^2 varied from -0.5 to 2. Calculations were carried out for magnetic fields of 9.4, 11.7, 14.1, and 18.8 T.

tered with axial-potential-based fitting, we subjected the ^{2}H T_1 and T_2 methyl relaxation rates of protein L to rhombic-potential-based SRLS fitting. The rationale for this enhancement is based on both statistical and physical considerations. As illustrated previously,[41,45−48] low χ^2 may be obtained with force fitting. Hence the fulfillment of statistical criteria is a necessary but insufficient condition. We require not only that χ^2 be low, which already has been accomplished by the axial-potential-based calculations of Table 1, but also that effects that have been shown to affect the analysis significantly, such as potential rhombicity, be accounted for. We also require reproduction of both the experimental ^{2}H autocorrelated relaxation rates and the experimental HC−HH cross-correlated rates, which are probing the same dynamic process. Finally, we require a physically

plausible temperature dependence of order parameters and correlation times. If all of these conditions are fulfilled, then the rhombic-potential-based results supersede the axial-potential-based results.

Uncertainties in the best-fit parameters are to be estimated. Choy and Kay[53] showed in the context of the MF approach that even when five synthetic ^{2}H relaxation rates generated at four magnetic fields are used as the experimental data set, the uncertainties in the best-fit parameters are very large. This is an intrinsic problem of ^{2}H methyl dynamics implied by sampling only a limited relatively low-frequency region of the spectral density.[53] Kay et al.[13] estimated parameter errors by systematically excluding subsets of data from the calculation. Adopting a similar strategy, we estimate the uncertainties in the best-fit SRLS parameters shown in Tables 1 and 5, and in general presented in this paper, to be on the order of 5%.

Table 5 shows the results of the rhombic-potential-based SRLS calculations. The parameters c_0^2, c_2^2, β_{MQ}, and $R^C/R^L = \tau^L/\tau_m$ were allowed to vary, with $\tau_m = 4.05$ ns from ref 13. This combination is the formal rhombic potential SRLS analogue of the model 5 MF approach. Relevant MF results from ref 13 are also shown. The parameter $c_0^2(MF)$ was calculated from S^2 using eqs 7 and 12. We recall that the axial coefficient, c_0^2, is a measure of the strength of the local potential whereas the rhombic coefficient, c_2^2, is a measure of the deviation from axial symmetry. Rhombicity at different sites can be compared based on c_2^2/c_0^2. It can be seen that τ^L/τ_m for the SRLS approach is generally larger than τ_e/τ_m for the MF approach, pointing out a smaller time scale separation in the SRLS as compared to the MF analysis. Note that the opposite trend was obtained for (oversimplified) axial potentials (Table 1). The average value of $\tau^L/\tau_m = 0.017$ in Table 5 is large enough for mode-coupling effects, ignored in the MF approach, to be important.[40−42]

20624 *J. Phys. Chem. B, Vol. 110, No. 41, 2006*

Meirovitch et al.

TABLE 5: Best-Fit Values of c_0^2, c_2^2, β_{MQ}, and τ^L/τ_m Obtained by Fitting the ^{2}H T_1 and T_2 Relaxation Rates of Protein L Acquired at 25 °C[12,13] with Rhombic SRLS Potentials[a]

residue	c_0^2	c_2^2	τ^L/τ_m	β_{MQ}	S_{axis}^2	c_0^2(MF)	τ_e/τ_m
				Group a			
T3	1.94	-0.70	0.016	70.4°	0.88	1.32	0.010
A11	1.89	-0.69	0.016	70.3°	0.89	1.36	0.012
T23	1.82	-0.67	0.017	70.2°	0.84	1.30	0.010
A50	1.88	-0.77	0.016	69.1°	0.84	1.30	0.006
I58γ	1.82	-0.74	0.016	69.1°	0.82	1.29	0.007
				Group b			
A18	1.06	-0.88	0.017	69.9°	0.81	1.28	0.014
A33	1.02	-0.91	0.018	69.2°	0.82	1.34	0.009
T55	1.17	-1.03	0.017	70.2°	0.98	1.40	0.012
				Group c			
T37	1.67	-0.63	0.017	70.5°	0.74	1.23	0.012
V49γ_1	1.65	-0.62	0.017	69.2°	0.68	1.17	0.008
I58δ	1.63	-0.58	0.017	67.7°	0.58	1.09	0.004
				Group d			
V49γ_2	1.56	-0.58	0.017	69.1°	0.62	1.13	0.010
L56δ_1	1.51	-0.35	0.017	72.2°	0.61	1.12	0.017
L56δ_2	1.57	-0.58	0.017	69.1°	0.61	1.12	0.009
A61	1.46	-0.56	0.017	69.5°	0.60	1.11	0.011
V47γ_1	1.28	-0.58	0.017	69.9°	0.57	1.08	0.014
L38δ_1	1.49	-0.49	0.018	68.7°	0.56	1.07	0.008
L38δ_2	1.35	-0.45	0.018	68.9°	0.47	0.98	0.010
				Remaining Methyl Groups			
I4γ	1.11	-0.97	0.011	68.7°	0.87	1.32	0.006
A6	1.38	-0.71	0.016	71.9°	0.80	1.27	0.018
I9γ	1.75	-0.71	0.016	69.2°	0.77	1.25	0.007
A35	2.00	+0.01	0.014	79.3°	0.80	1.27	0.033
V2γ_1	1.60	-0.62	0.017	70.4°	0.73	1.22	0.013
V2γ_2	1.52	-0.58	0.017	69.3°	0.64	1.14	0.010
T15	1.59	-0.25	0.018	71.5°	0.57	1.08	0.017
T46	1.39	-0.57	0.015	70.9°	0.69	1.18	0.016
V47γ_2	0.76	-0.72	0.015	72.6°	0.66	1.16	0.019

[a] The global motion correlation time used was $\tau_m = 4.05$.[13] The S_{axis}^2 and τ_e/τ_m values obtained with the MF analysis[13] and c_0^2(MF) derived from S^2 using eqs 7 and 12 are also shown. The χ^2 values of the SRLS calculations are typically below 2. The classification into groups a–d is based on S_{axis}^2 values, as outlined in the text.

TABLE 6: Average c_0^2 and c_2^2 Values Corresponding to Groups a–d[a]

group	$\langle c_0^2 \rangle$	$\langle c_2^2 \rangle$	c_2^2/c_0^2	$\langle S_{xx} \rangle$	$\langle S_{yy} \rangle$	$\langle S_{zz} \rangle$
a	1.87	-0.71	-0.38	-0.275	-0.114	+0.389
b	1.08	-0.94	-0.87	-0.249	+0.060	+0.189
c	1.65	-0.61	-0.37	-0.251	-0.097	+0.348
d	1.46	-0.51	-0.35	-0.226	-0.085	+0.311

[a] Cartesian ordering tensor components S_{xx}, S_{yy}, and S_{zz} were calculated from $\langle c_0^2 \rangle$ and $\langle c_2^2 \rangle$ via S_0^2 and S_2^2, as outlined in the text.

The data shown in Table 5 were classified according to the value of S_{axis}^2, which was determined in ref 13. Group a comprises methyl groups with high S_{axis}^2, comparable c_0^2(SRLS), and comparable c_2^2(SRLS) values. Group d comprises methyl groups with relatively low S_{axis}^2, comparable c_0^2(SRLS), and comparable c_2^2(SRLS) values. Groups b and c comprise methyl groups with comparable c_0^2(SRLS), comparable c_2^2(SRLS), and diverse S_{axis}^2 values. The last group in Table 5 comprises the remaining methyl groups.

The coefficients of the *average* potentials corresponding to groups a–d, $\langle c_0^2 \rangle$, and $\langle c_2^2 \rangle$, are given in Table 6. It can be seen that $\langle c_0^2 \rangle$ of group a, which corresponds to high S_{axis}^2, differs from $\langle c_0^2 \rangle$ of group d, which corresponds to relatively low S_{axis}^2, by 13.3%. From $\langle c_0^2 \rangle$ and $\langle c_2^2 \rangle$, we calculated the irreducible ordering components, $\langle S_0^2 \rangle$ and $\langle S_2^2 \rangle$ (eqs 7 and 12), and from

TABLE 7: Best-Fit Parameters Obtained for the Methyl Groups I4δ, T14, L8δ_1, and L8δ_2 of Protein L and Cartesian Ordering Tensor Components S_{xx}, S_{yy}, and S_{zz} Derived from c_0^2 and c_2^2 [a]

residue	c_0^2	c_2^2	τ^L/τ_m	β_{MQ}	χ^2	S_{xx}	S_{yy}	S_{zz}
I4δ	1.43	-0.27	0.018	68.2°	12.3	-0.195	-0.119	+0.315
T17	1.48	-0.34	0.016	72.5°	4.6	-0.208	-0.115	+0.323
L8δ_1	1.15	1.00	0.017	68.1°	31.0[a]	+0.060	-0.259	+0.199
L8δ_2	0.95	1.00	0.017	67.5°	14.7	+0.097	-0.248	+0.152

[a] Methyl L8δ_1 may require further investigation in view of the high χ^2 value.

these values the Cartesian tensor components, $\langle S_{xx} \rangle$, $\langle S_{yy} \rangle$, and $\langle S_{zz} \rangle$, were derived. The latter quantities are also shown in Table 6. The largest absolute value among the Cartesian ordering tensor components is $|\langle S_{zz} \rangle| = 0.389$ for group a and $|\langle S_{zz} \rangle| = 0.311$ for group d, differing by 20%. Both $\langle c_0^2 \rangle$ and $|\langle S_{zz} \rangle|$ estimate the strength of the local spatial restrictions at the site of the motion of the methyl group. In the MF approach these restrictions are evaluated by S_{axis}^2, which is 0.854 for group a and 0.577 for group d. These values differ by 48%, *highlighting the significant* overestimation of the actual variations in the local ordering by S_{axis}^2.

The ratio c_2^2/c_0^2 is a measure of potential rhombicity. Although the average values, $\langle c_2^2 \rangle/\langle c_0^2 \rangle$, are similar for groups a, c, and d (Table 6), the c_2^2/c_0^2 values of the individual methyl groups within the most sensitive group d differ by up to a factor of 2.5. Group b features a $\langle c_2^2 \rangle/\langle c_0^2 \rangle$ value different from the other groups. There are considerable variations in the symmetry of the local potential among the members of this group. In the last category shown in Table 5, some methyl groups feature the dominant symmetry while others feature different symmetries. For example, A35 is associated with $c_2^2/c_0^2 \approx 0$, T15 with $c_2^2/c_0^2 = 0.16$, V47γ_2 with $c_2^2/c_0^2 = 0.95$, and A6 with $c_2^2/c_0^2 = 0.51$. It is obvious that *the symmetry of the local* restrictions is an important aspect of methyl dynamics.

It is of interest to consider the four methyl groups of protein L that required special treatment in the MF analysis.[13] The best-fit SRLS parameters for these methyl groups are shown in Table 7 together with the Cartesian tensor components corresponding to c_0^2 and c_2^2. With a somewhat lenient χ^2 threshold, the methyl groups of residues I4δ and T17 can be considered fit with the same type of potential symmetry as most methyl groups. The methyl groups of residue L8 were fit with large negative S_{yy}, large positive S_{zz}, and small S_{xx}. This represents "nearly planar Y_M–Z_M ordering", the meaning of which should be further explored. Note that the SRLS approach is able to interpret the data of all the methyl groups of protein L with the same model but different symmetry of the local ordering, whereas in the MF approach different models had to be used for methyl groups I4δ, T17, L8δ_1, and L8δ_2.

Let us discuss the physical meaning of the rhombic potentials/rhombic ordering determined by the SRLS analysis. The ordering tensor is diagonal in the M frame. The orientation of the C−D bond (Z_Q axis) in this frame is given by the angles β_{MQ} and γ_{MQ}. Note that the fitting scheme yields $\beta_{MQ} \approx 70°$ while the tetrahedral angle is 110.5°. The time correlation function is the same for β_{MQ} and $180° - \beta_{MQ}$. The minimization routine converges for numerical reasons to $\beta_{MQ} \approx 70°$, which can be taken to represent $\beta_{MQ} \approx 110°$. The absolute values of the Cartesian tensor components, S_{xx}, S_{yy}, and S_{zz}, express the extent to which the principal axes, X_M, Y_M, and Z_M, align preferentially either parallel (for positive components) or perpendicular (for negative components) to the local director,
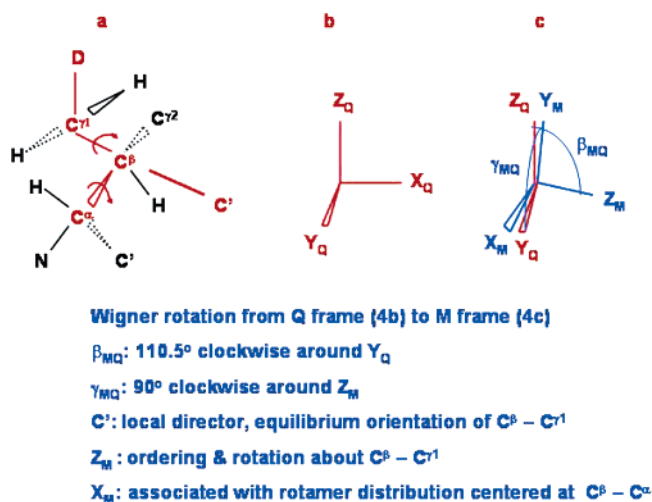
SRLS/NMR Analysis of Methyl Dynamics in Proteins

J. Phys. Chem. B, Vol. 110, No. 41, 2006 **20625**

Figure 4. Illustration of the local ordering/local diffusion frame, M, corresponding to a valine $C^{\gamma}H_2D$ methyl group. For methyl rotation the angle between Z_M and C—D is 110.5° (with $r_{CH} = r_{CD} = 1.115$ Å). By setting γ_{MD} equal to 90° one obtains an M frame that is physically meaningful, as outlined in the text.

C'. The latter is a structural entity fixed in the protein relative to which ordering occurs. For example, in the 3D GAF model[57] the C^{α}_{i-1}—C^{α}_i axis is taken as the local director for N—H motion. Note that the angle between the N—H bond and the C^{α}_{i-1}—C^{α}_i axis is fixed in the 3D GAF model. It is reasonable to associate C' for methyl rotation with the C(methyl)—C bond, as depicted in Figure 1b. Unlike the 3D GAF model, the SRLS model allows for β_{MD} and γ_{MD} to be varied.

The local ordering and local diffusion frames are taken to be the same in the SRLS approach. Hence, X_M, Y_M, and Z_M are both ordering and diffusion axes. The relation between the magnetic frame, Q, the local ordering/local diffusion frame, M, and the local director frame, C', is illustrated for a valine methyl, $^{13}C^{\gamma}1H_2D$, in Figure 4a. The magnetic quadrupolar frame, Q, with Z_Q along the C—D bond, is shown in Figure 4b. A clockwise rotation of $\beta_{MQ} = 110.5°$ about Y_Q and a subsequent clockwise rotation of $\beta_{MQ} = 90°$ about the new Z axis (the Wigner convention of left-handed coordinate frames is used) yield the (rhombic) M frame shown in Figure 4c. Z_M lies along the instantaneous orientation of the C^{β}—$C^{\gamma 1}$ bond and is tilted at an angle $\beta_{MQ} = 110.5°$ relative to the C—D bond. X_M lies close to the instantaneous orientation of the C^{β}—C^{α} bond, and Y_M lies close to the instantaneous orientation of the C^{β}—$C^{\gamma 2}$ bond. The local director, C', is taken to lie along the equilibrium orientation of the C^{β}—$C^{\gamma 1}$ bond.

Z_M represents the diffusion axis for methyl rotation about C^{β}—$C^{\gamma 1}$ and the ordering axis associated with this dynamic mode. X_M may be associated with fast rotameric transitions about the dihedral angle C'—C^{α}—C^{β}—$C^{\gamma 1}$. R^C/R^L is practically constant for the methyl groups of protein L, in support of the rates of these transitions being in the extreme motional narrowing limit. As pointed out above, the form of the local potential and the local ordering tensor correlates with the relative population of rapidly interconverting side-chain rotamers. This is illustrated empirically in the next section for RDC-based populations. Clearly it is of interest to compare directly spin-relaxation-derived populations with those determined with other experimental (e.g., J-coupling and RDC) and theoretical (MM and MD) methods. For that, the SRLS approach needs to be extended to comprise detailed treatment of side-chain flexibility. Such developments are in progress.[49−51]

1. Rotamer Population Distribution around χ_1 in Protein L.[31] We found that the population distribution around the dihedral angle χ_1 determined for protein L from dipolar couplings[31] can be correlated with S_{xx}, S_{yy}, and S_{zz} yielded by the SRLS analysis. This is illustrated in Table 8 where relative populations given in ref 31 for the methyl groups of residues T28, T37, T15, T46, T3, I9, L56, and L38 are shown along with the best-fit c_0^2 and c_2^2 values and corresponding Cartesian ordering tensor components obtained with the SRLS approach. The ordering tensors differ mainly in the magnitude of S_{yy}. This component is relatively large for T28, T15, and T3, where the dominant rotamer is tr or g− (italic type), and relatively small for T37 and T46, where the dominant rotamer is g+ (boldface type). S_{yy} is relatively small for all the Ile and Leu methyl groups for which the dominant rotameric state is g− (boldface and italic type). These results are interesting and warrant further investigation beyond the correlations that have been pointed out. Through the use of the strategy of ref 49, torsional potentials should be calculated (using quantum chemical methods) for all the bonds in the side chain, the ensemble of ensuing conformers should be pruned based on some measure for the steric effect of the environment, and finally the P_{eq} function should be derived. The latter quantity could be used to derive a mean-field potential similar to the SRLS potential. Alternatively, an approximate P_{eq} function could be obtained from MD or Monte Carlo simulations. The integrated approach presented in ref 51 is designed in this spirit and will be applied shortly to methyl dynamics in proteins.

2. $\eta_{HC−HH}$ Cross-Correlation in Protein L.[18] Unlike all of the previous SRLS and MF models based on axial potentials, which could only reproduce ^{2}H relaxation and $\eta_{HC−HH}$ cross-correlation with spectral densities featuring different parameter combinations, the rhombic-potential-based SRLS model satisfactorily reproduces the two types of relaxation rates with the same spectral density. This is shown in Table 9, which features the experimental $\eta_{HC−HH}$ values from ref 18 acquired at 25 °C and the corresponding $\eta_{HC−HH}$ values (given by $J(0)$) calculated with the best-fit parameters yielded by the ^{2}H relaxation analysis of Table 5. The value of $\tau_m = 4.05$ ns (H_2O solution)[12,13] was used in ^{2}H fitting, and $\tau_m = 5.0$ ns (D_2O solution)[18] was used to calculate $\eta_{CH−HH}$. The ability to carry out successfully combined analyses of auto- and cross-correlated relaxation rates only when the local potential/local ordering is allowed to be rhombic points out the key role of the symmetry of the potential in the analysis of methyl dynamics. Since rhombic ordering is outside the scope of the MF approach, the analysis of different relaxation rates, using the same parameter combination, is not successful because force fitting is scenario-dependent.

It was found by Tugarinov and Kay[18] that at 45 °C S^2_{axis} values calculated from the experimental $\eta_{HC−HH}$ values significantly exceed S^2_{axis} values from ^{2}H relaxation analysis.[12,13] Furthermore, above 25 °C S^2_{axis} obtained from $\eta_{HC−HH}$ was found to *increase* with increasing temperature.[18] For axial local potentials, the SRLS approach can also reproduce the 45 °C $\eta_{HC−HH}$ rates only with local ordering that is *higher* than the ordering obtained at 25 °C (data not shown). This situation changes when the symmetry of the local potential/ local ordering is allowed to be rhombic. Row 1 of Table 10 shows $\eta_{HC−HH}$ obtained for methyl group V49γ_1 using the best-fit parameters from the ^{2}H analysis at 25 °C. Preserving the local geometry (the angle β_{MQ}) and the ratio τ^L/τ_m (i.e., assuming that τ^L and τ_m are associated with comparable activation energies) and using $\tau_m = 2.1$ ns obtained with ^{15}N relaxation at 45° C,[18] it is possible to reproduce the experimental value of $\eta_{HC−HH}$ of V49γ_1

TABLE 8: Protein L Methyl Groups for which Mittermaier and Kay[31] Determined the Rotamer Population Distribution around the Dihedral Angle χ_1 from Dipolar Couplings

					^{2}H best-fit parameters						
	pg+	ptr	pg–	S^2_{axis}	c^2_0	c^2_2	τ^L/τ_m	β_{MQ}	S_{xx}	S_{yy}	S_{zz}
T28	0.28	0.19	*0.53*	0.88	2.05	−0.65	0.016	70.9°	−0.282	*−0.148*	0.430
T37	**0.60**	0.11	0.30	0.74	1.67	−0.63	0.017	70.5°	−0.254	**−0.096**	0.351
T15	0.21	*0.66*	0.13	0.57	1.60	−.30	0.018	71.5°	−0.214	*−0.137*	0.354
T46	**0.74**	0.12	0.14	0.69	1.40	−0.60	0.017	70.9°	−0.232	**−0.060**	0.292
T3	0.06	0.03	*0.91*	0.88	1.94	−0.70	0.016	70.4°°	−0.279	*−0.126*	0.404
I9g	0.06	0.07	**0.87**	0.77	1.75	−0.71	0.016	69.2°	−0.267	**−0.096**	0.363
L56d1	0.06	0.01	**0.93**	0.61	1.51	−0.35	0.017	72.2°	−0.212	**−0.118**	0.330
L56d2	0.06	0.01	**0.93**	0.61	1.57	−0.58	0.017	69.1°	−0.242	**−0.090**	0.332
L38d1	0.01	0.08	**0.91**	0.56	1.49	−0.49	0.018	68.7°	−0.226	**−0.092**	0.319
L38d2	0.01	0.08	**0.91**	0.47	1.35	−0.45	0.018	68.9°	−0.210	**−0.079**	0.289

TABLE 9: η_{HC-HH} Calculated Based on $J(0)$ (Eq 2 of Ref 18) Using the Best-Fit Parameters Yielded by the ^{2}H Analysis Given in Table 5[a]

residue	η_{HC-HH}(exptl), s^{-1}	η_{HC-HH}(calcd), s^{-1}
V2g1	24.7 ± 0.6	25.1
V2g2	22.6 ± 0.5	21.2
V47g1	20.5 ± 0.6	20.8
V47g2	23.3 ± 0.6	24.3
V49g1	23.7 ± 0.6	22.7
V49g2	21.3 ± 0.5	21.0
I4d	12.0 ± 0.1	12.25
L8d1	5.9 ± 0.1	7.4
L8d2	6.7 ± 0.1	10.2
I9d	13.7 ± 0.1	13.3
L38d1	17.8 ± 0.2	18.0
L38d2	16.2 ± 0.2	16.6
L56d1	20.3 ± 0.4	21.8
L56d2	20.2 ± 0.4	21.1
I58d	20.2 ± 0.2	18.2

[a] The experimental η_{HC-HH} data were taken from Table 1 of ref 18.

TABLE 10: (Row 1) Best-Fit c^2_0 and c^2_2 Values, Obtained by Fitting the ^{2}H Relaxation Data of V49γ_1 Acquired at 25 °C, and η_{HC-HH} Value Calculated with These Parameters and (Rows 2 and 3) c^2_0 and c^2_2 Values that Reproduce the η_{HC-HH} Value of V49γ_1 at 45 °C and that Are Smaller Than c^2_0 and c^2_2 of Row 1[a]

temp, °C	c^2_0	c^2_2	S_{xx}	S_{yy}	S_{zz}	η_{HC-HH}
25	+1.65	−0.62	−0.252	−0.095	+0.347	22.7 (23.7)
45	+1.40	−1.09	−0.234	−0.057	+0.291	13.7 (13.7)
45	−1.00	+0.60	+0.270	−0.087	−0.183	13.7 (13.7)

[a] β_{MQ} = 69.2° and τ^L/τ_m = 0.017, obtained at 25 °C, were used to obtain the results shown in rows 2 and 3. The η_{HC-HH} values in parentheses are the experimental values reported in ref 18. The components of the Cartesian tensor calculated from c^2_0 and c^2_2 are also shown.

measured at 45 °C with *lower potentials*. This is shown in rows 2 and 3 of Table 10, which feature examples of parameter sets with diminished ordering. To pinpoint the particular parameter set that reproduces *both* ^{2}H relaxation and η_{HC-HH} cross-correlation at 45 °C, SRLS analysis of the experimental ^{2}H relaxation rates acquired at 45 °C is yet to be performed.

The discrepancies between S^2_{axis} from ^{2}H relaxation and η_{HC-HH} cross-correlation at 45 °C may be related qualitatively to the effect of τ_e on the MF analysis. At this temperature, where τ_m = 2.1 ns,[18] one has $J(2\omega_D) \approx J(\omega_D) \approx J(0)$. Hence, similar to ^{2}H T_2 and η_{HC-HH}, ^{2}H T_1 is also given predominantly by $J(0)$, i.e., by S^2_{axis}, with τ_e thus affecting the analysis marginally. The parametrization of the experimental spectral density in terms of S^2_{axis} and τ_e, which was effective at 25° C, is no

TABLE 11: Typical Best-Fit Parameters Obtained with SRLS Analysis of the ^{2}H T_1 and T_2 Ubiquitin Data of Lee et al.[8] and the Corresponding Best-Fit MF Parameters[8] [a]

residue	c^2_0	c^2_2	τ^L/τ_m	β_{MQ}	S^2_{axis}	c^2_0(MF)	τ_e/τ_m
			Group a				
V5g1	0.17	0.95	0.001	72.2°	0.83	1.36	0.010
V5g2	−0.19	0.82	0.016	67.2°	0.80	1.34	0.005
T70	0.18	0.90	0.017	68.9°	0.68	1.24	0.012
T12	−0.04	0.89	0.016	68.5°	0.85	1.38	0.010
I30g	0.05	0.89	0.017	65.9°	0.85	1.30	0.007
I36g	0.18	0.90	0.017	72.3°	0.75	1.29	0.021
			Group b				
T9	0.28	0.90	0.017	67.4°	0.59	1.15	0.009
I13d	0.37	0.90	0.017	66.0°	0.50	1.08	0.011
I36d	0.32	0.90	0.017	66.0°	0.53	1.10	0.006
L43d1	0.44	0.90	0.017	69.9°	0.50	1.07	0.016
L15d1	0.35	0.90	0.017	67.4°	0.53	1.10	0.009
			Group c				
L8d1	0.80	0.91	0.017	68.0°	0.24	0.75	0.012
L8d2	0.91	0.91	0.017	67.9°	0.19	0.68	0.012
L67d1	0.75	0.91	0.017	68.9°	0.27	0.80	0.015
L67d2	0.77	0.91	0.017	67.9°	0.26	0.79	0.012
L73d2	0.98	0.91	0.017	67.1°	0.15	0.61	0.010

[a] c^2_0(MF) was derived from S^2 using the potential $u = -c^2_0 P_2 \times (\cos \beta_{CM})$ (eqs 7 and 12).

longer appropriate at 45 °C. Minima with low χ^2 can only be obtained at 45 °C with unduly large force-fitted S^2_{axis} values.

B. Ubiquitin.[8] Wand and co-workers studied ^{2}H relaxation of ^{13}CH$_2$D groups in ubiquitin using the MF approach.[8] Data were acquired at 14.1 and 17.6 T and 30°C. A three-pronged distribution in S^2_{axis} was obtained.

We subjected the ubiquitin data[8] to SRLS analysis. Table 11 shows typical best-fit parameters obtained with rhombic-potential-based SRLS fitting, along with the MF results. The coefficient c^2_0(MF) was calculated from S^2(MF) using the potential $u = -c^2_0 P_2(\cos \beta_{CM})$ (eqs 7 and 12). Group a corresponds to methyl groups with high S^2_{axis} values ($\langle S^2_{axis} \rangle$ = 0.79), group b to methyl groups with S^2_{axis} of medium magnitude ($\langle S^2_{axis} \rangle$ = 0.53), and group c to methyl groups with low S^2_{axis} values ($\langle S^2_{axis} \rangle$ = 0.22).

The parameter τ^L/τ_m of the SRLS approach is on average larger than τ_e/τ_m of the MF approach, pointing out a smaller time scale separation determined by the SRLS analysis. The τ^L/τ_m values are significantly more uniform than the τ_e/τ_m values (V5γ_1 in an outlier in the SRLS analysis). The average c^2_0 and c^2_2 values of groups a−c and the corresponding Cartesian ordering tensor components are shown in Table 12. Nearly planar ordering prevails for all the groups, the difference consisting in which axes form the "plane", and which is the main ordering axis. Group a is characterized by positive S_{xx},

TABLE 12: Average c_0^2 and c_2^2 Values of (a) 13 Ubiquitin Residues with $S_{axis}^2 > 0.85$, (b) Ubiquitin Residues I13γ, T9, I13δ, I23δ, and I36δ with $0.55 < S_{axis}^2 < 0.65$, and (c) Ubiquitin Residues L8δ_1, L8δ_2, L67δ_1, L67δ_2, V70γ, L71δ_1, and L73δ_2 with $S_{axis}^2 < 0.3^a$

group	$\langle c_0^2 \rangle$	$\langle c_2^2 \rangle$	$\langle c_2^2 \rangle / \langle c_0^2 \rangle$	$\langle S_{xx} \rangle$	$\langle S_{yy} \rangle$	$\langle S_{zz} \rangle$
a	0.06	0.89	14.8	+0.221	−0.190	−0.030
b	0.35	0.90	2.6	+0.178	−0.205	+0.028
c	0.84	0.91	1.1	+0.096	−0.232	+0.136

^{a} In all the cases considered the best-fit angle β_{MQ} was close to 70°. The calculation of $\langle S_{xx} \rangle$, $\langle S_{yy} \rangle$, and $\langle S_{zz} \rangle$ from $\langle c_0^2 \rangle$ and $\langle c_2^2 \rangle$ was carried out as outlined in the text.

negative S_{yy} with a similar absolute value as S_{xx}, and small negative S_{zz}. $|S_{xx}|$ is the largest absolute value. This is nearly planar $X_M - Y_M$ ordering with X_M as the main ordering axis. On the basis of analogous reasoning, group b is associated with nearly planar $Y_M - X_M$ ordering with Y_M as main ordering axis, and group c with nearly planar $Y_M - Z_M$ ordering with Y_M as the main ordering axis. *Thus, the three-pronged distribution in experimental data is interpreted with the SRLS model in terms of three types of rhombic potential symmetries.*

On the basis of $\langle c_2^2 \rangle / \langle c_0^2 \rangle$ values group a features very high potential rhombicity, group b features moderate rhombicity, and group c features small rhombicity. Further studies of the local potential/local ordering, including contributions from fast side-chain rotamer jumps,[49−51] are clearly warranted. It is certainly of interest to use rhombic potentials to derive residual conformational entropy.

C. Local Potentials/Local Ordering, Residual Configurational Entropy, etc. *1. Local Potentials/Local Ordering.* The principal values of ordering tensors are determined by structural, electronic, and charge-related properties of the probe engaged in restricted motion and the environment which exerts the restrictions. This is the established view when the environment is a liquid-crystalline solvent[58] or a weakly orienting medium used to measure residual dipolar coupling in proteins.[59]

The SRLS model[42,43] is an extension of established single-body models for restricted motion in locally ordered media, with the static liquid-crystalline director replaced in the SRLS approach by a protein-fixed local director that typically "relaxes slowly" with respect to the fixed lab frame. The potential coefficients c_0^2 and c_2^2, the principal values S_0^2 and S_2^2 of the irreducible ordering tensor or the principal values S_{xx}, S_{yy}, and S_{zz} of the Cartesian ordering tensor, preserve their established meaning.[58,59] The immediate internal protein surroundings of the dynamic probe play the role of the locally ordered solvent.[43] Thus, the SRLS-determined local potentials and local ordering tensors comprise important structural information that is yet to be related to protein function.

Note that ordering potentials are the generic physical quantities that enter dynamic models for restricted motions.[42−44] Order parameters are ensemble averages defined in terms of ordering potentials. Using squared order parameters as weighting factors in the spectral density is only valid in the limit where $\tau^L/\tau_m \ll 1$, when the local potential is either very low (perturbation limit)[52,56] or very high (BO limit[55]).[40,41] Interpreting squared order parameters as motional amplitudes is only valid in the limit where $\tau^L/\tau_m \ll 1$ when the local ordering is axially symmetric and high, as only in this case can they be taken to represent the mean-squared amplitude of all the internal motions.[44]

2. Residual Configurational Entropy. Backbone and side-chain order parameters are often used to calculate residual configurational entropy.[36−39] This requires the equilibrium probability distribution function, P_{eq}, given by the local potential

that restricts the motion of the dynamic probe. The MF formalism does not feature local potentials explicitly. For methyl dynamics S_{axis}^2 is first determined with data fitting. Then a specific potential form, which must be axially symmetric since only one order parameter is available, is suggested, and its coefficient is derived from S_{axis} by expressing the latter as an ensemble average. The potential thus determined is inserted into the expression for P_{eq}, and residual configurational entropy is calculated. If S_{axis}^2 is inaccurate and its variation overextended because of the various MF simplifications outlined above, so will be the NMR-derived local potential, hence the residual configurational entropy. Moreover, some potential forms used in the MF approach may be inconsistent with cosine squared potentials for which a physically meaningful "renormalized" local motion correlation time prevails in the BO limit.[40,55] In such cases, the form of eq 2, hence eq 4, will be inappropriate.[41]

In the SRLS approach the local potential is intrinsic to the model. Its form is as general in nature as practically feasible. In the current implementation $L = 2$ terms of the complete expansion in Wigner rotation matrix elements have been preserved (eq 7). With the coefficients c_0^2 and c_2^2 determined by data fitting, residual configurational entropy is an automatic byproduct of the analysis.

3. Further Comments. The following comments are in order. The contact model of Ming and Bruschweiler[35] reproduces well most of the experimental S_{axis}^2 values[13] of protein L. The latter are quite high, being apparently dominated by packing effects which are captured by the contact model. For other proteins the correspondence between theory and experiment in ref 35 is less satisfactory.

In the SRLS approach "mode coupling" means that by virtue of the local spatial restrictions exerted by the immediate protein surroundings at the site of the motion of the dynamic probe, the latter reorients with respect to these surroundings, which themselves reorient at a slower rate with respect to a fixed lab frame. The motion of the probe involves the variables of both probe and protein, whereas the motion of the protein involves only the variables of the protein. "Mode decoupling" means that the local motion can be treated for frozen global motion. This is totally different from the concept of "separability" between global and local motion modes, based on the analysis of the covariance matrix of spherical harmonic functions of rank 2, which is a geometric notion.[60−62] Modes that are not "separable" are by no means "coupled" or "mixed" dynamically, as implied in some cases.[63]

A new protocol for the experimental determination of ensembles of protein conformations that represent simultaneously the native structure and its associated dynamics was set forth recently.[64] This method uses experimental NMR order parameters determined with the MF approach and theoretical order parameters calculated from MD trajectories as outlined in ref 28. We have shown that MF-derived order parameters are typically inaccurate. The authors of ref 30 have shown that the method of ref 28 is oversimplified, leading to inaccurate order parameters. It would be of interest to apply this protocol using experimental order parameters determined with the SRLS approach and theoretical order parameters determined as outlined in ref 30. Even better, one could use experimental potential coefficients determined with the SRLS approach and theoretical potentials of mean force calculated as outlined in ref 39.

IV. Conclusions

SRLS analysis of methyl dynamics in proteins indicates that the local ordering potentials at the site of the motion of the

methyl group are rhombic. The diversity of the experimental data stems primarily from variations in the symmetry of the local potential/local ordering and to some extent its strength. The methyl averaging axis is tilted relative to the C−D bond at approximately 110.5°, as determined with data fitting. The time scale separation between the local and the global motions is on the order of 0.02. This value is large enough for mode coupling to be important. The form of the SRLS local coupling/ordering potential has been correlated with RDC-derived populations of rapidly interconverting side-chain rotamers. The SRLS approach can analyze in concert consistently ^{2}H autocorrelated relaxation in $^{13}CH_2D$ methyl groups and η_{CH-HH} cross-correlated relaxation in their $^{13}CH_3$ counterparts. Residual configurational entropy based on experimentally determined rhombic potentials is an automatic byproduct of the SRLS analysis.

Important effects associated with mode coupling, asymmetric ordering, and general features of local geometry are either ignored or oversimplified in the MF approach. While S^2 is itself a parametrizing entity, for methyl dynamics it is further parametrized as $0.1S_{axis}^2$. The squared order parameters S_{axis}^2 are inaccurate, and their distribution overestimates the actual variations in the spatial restrictions at the site of the motion of the methyl group. Parametrization implies inconsistencies in combined analyses of different methyl-related relaxation rates. S_{axis}^2 is interpreted as "amplitude of motion". This interpretation is only valid in the extreme motional narrowing limit where $\tau_e \approx 0$, and its axiality is inconsistent with the local asymmetry shown by MD and RDC studies to be important in explaining NMR-derived order parameters.

References and Notes

(1) Kay, L. E. *Nat. Struct. Biol.* **1998**, *5*, 513−517.

(2) Ishima, R.; Torchia, D. A. *Nat. Struct. Biol.* **2000**, *7*, 740−743.

(3) Palmer, A. G., III. *Chem. Rev.* **2004**, *104*, 3623−3640.

(4) Case, D. *Acc. Chem. Res.* **2002**, *35*, 325−333.

(5) Bruschweiler, R. *Curr. Opin. Struct. Biol.* **2003**, *13*, 175−183.

(6) Nicholson, L. K.; Kay, L. E.; Baldisseri, D. M.; Arango, J.; Young, P. E.; Bax, A.; Torchia, D. A. *Biochemistry* **1992**, *31*, 5253−5263.

(7) Mittermaier, A.; Kay, L. E.; Forman-Kay, J. D. *J. Biomol. NMR* **1999**, *13*, 181−185.

(8) Lee, A. L.; Flynn, P. E.; Wand, A. J. *J. Am. Chem. Soc.* **1999**, *121*, 2891−2902.

(9) Mayer, K. L.; Early, M. R.; Gupta, S.; Pichumani, K.; Regan, L.; Stone, M. J. *Nat. Struct. Biol.* **2003**, *10*, 962−965.

(10) Schnell, J. R.; Dyson, H. J.; Wright, P. E. *Biochemistry* **2004**, *43*, 374−383.

(11) Muhandiram, D. R.; Yamazaki, T.; Sykes, B. D.; Kay, L. E. *J. Am. Chem. Soc.* **1995**, *117*, 11536−11544.

(12) Millet, O.; Muhandiram, D. R.; Skrynnikov, N. R.; Kay, L. E. *J. Am. Chem. Soc.* **2002**, *124*, 6439−6448.

(13) Srynnikov, N, R.; Millet, O.; Kay, L. E. *J. Am. Chem. Soc.* **2002**, *124*, 6449−6460.

(14) Kay, L. E.; Bull, T. E.; Nicholson, L. K.; Griesinger, C.; Schwalbe, H.; Bax. A.; Torchia, D. A. *J. Magn. Reson.* **1992**, *100*, 538−558.

(15) Kay, L. E.; Torchia, D. A. *J. Magn. Reson.* **1991**, *95*, 536.

(16) Ishima, R.; Petkova, A. P.; Louis, J. M.; Torchia, D. A. *J. Am. Chem. Soc.* **2001**, *123*, 6164−6171.

(17) Tugarinov. V.; Kay, L. E. *Biochemistry* **2005**, *44*, 15970−15977.

(18) Tugarinov. V.; Kay, L. E. *J. Biomol. NMR* **2004**, *29*, 369−376.

(19) Lipari, G.; Szabo, A. *J. Am. Chem. Soc.* **1982**, *104*, 4546−4559.

(20) Lipari, G.; Szabo, A. *J. Am. Chem. Soc.* **1982**, *104*, 4559−4570.

(21) Clore, G. M.; Szabo, A.; Bax, A.; Kay, L. E.; Driscoll, P. C.; Gronenborn, A. M. *J. Am. Chem. Soc.* **1990**, *112*, 4989−4991.

(22) Mandel, A. M.; Akke, M.; Palmer, A. G., III. *J. Mol. Biol.* **1995**, *246*, 144−163.

(23) Fushman, D.; Cahill, S.; Cowburn, D. *J. Mol. Biol.* **1997**, *266*, 173−194.

(24) Chatfield, D. C.; Szabo, A.; Brooks, B. R. *J. Am. Chem. Soc.* **1998** *120*, 5301−5311.

(25) Lee, A. L.; Sharp, K. A.; Kranz. J. K.; Song, X.-J.; Wand, J. *Biochemistry* **2002**, *41*, 13814−13825.

(26) Lee, A. L.; Wand, A. J. *Nature* **2001**, *411*, 501−504.

(27) Prabhu, N. V.; Lee, A. L.; Wand. H.; Sharp, K. A. *Biochemistry* **2003**, *42*, 562−570.

(28) Henry, E.; Szabo, A. *J. Chem. Phys.* **1985**, *82*, 4753−4761.

(29) Best, R. B.; Clarke, J.; Karplus, M. *J. Am. Chem. Soc.* **2004**, *126*, 7734−7735.

(30) Best, R. B.; Clarke, J.; Karplus, M. *J. Mol. Biol.* **2005**, *349*, 185−203.

(31) Mittermaier, A.; Kay, L. E. *J. Am. Chem. Soc.* **2001**, *123*, 6892−6903.

(32) Chou, J. J.; Case, D. A.; Bax, A. *J. Am. Chem. Soc.* **2003**, *125*, 8959−8966.

(33) Hu, A.; Hermans, J.; Lee, A. L. *J. Biomol. NMR* **2005**, *32*, 151−162.

(34) Zhang, F.; Bruschweiler, R. *J. Am. Chem. Soc.* **2002**, *124*, 12654−12655.

(35) Ming, D.; Bruschweiler, R. *J. Biomol. NMR* **2004**, *29*, 363−368.

(36) Akke, M.; Bruschweiler, R.; Palmer, A. G., III. *J. Am. Chem. Soc.* **1993**, *115*, 9832−9833.

(37) Yang, D.; Kay, L. E. *J. Mol. Biol.* **1996**, *263*, 369−382.

(38) Lee, A. L.; Kinnear, S. A.; Wand, A. J. *Nat. Struct. Biol.* **2000**, *7*, 72−77.

(39) Massi, F.; Palmer, A. G., III. *J. Am. Chem. Soc.* **2003**, *125*, 11158−11159.

(40) Meirovitch, E.; Shapiro, Y. E.; Liang, Z.; Freed, J. H. *J. Phys. Chem. B* **2003**, *107*, 9898−9904.

(41) Meirovitch, E.; Shapiro. Y. E.; Polimeno. A.; Freed, J. H. *J. Phys. Chem. A* **2006**, *110*, 8366−8396.

(42) Polimeno, A.; Freed, J. H. *Adv. Chem. Phys.* **1993**, *83*, 89−210.

(43) Polimeno, A.; Freed, J. H. *J. Phys. Chem.* **1995**, *99*, 10995−11006.

(44) Liang, Z.; Freed, J. H. *J. Phys. Chem. B* **1999**, *103*, 6384−6396.

(45) Tugarinov, V.; Liang, Z.; Shapiro, Yu. E.; Freed, J. H.; Meirovitch, E. *J. Am. Chem. Soc.* **2001**, *123*, 3055−3063.

(46) Tugarinov, V.; Shapiro, Yu. E.; Liang, Z.; Freed, J. H.; Meirovitch, E. *J. Mol. Biol.* **2002**, *315*, 171−186.

(47) Shapiro, Yu. E.; Kahana E.; Tugarinov, Liang, Z.; Freed, J. H.; Meirovitch, E. *Biochemistry* **2002**, *41*, 6271−6281.

(48) Meirovitch, E.; Shapiro, Yu. E.; Tugarinov, V.; Liang, Z.; Freed, J. H. *J. Phys. Chem. B* **2003**, *107*, 9883−9897.

(49) Tombolato, F.; Ferrarini, A.; Freed, J. H. Dynamics of the nitroxide side-chain in spin labeled proteins *J. Phys. Chem.*, submitted for publication.

(50) Tombolato, F.; Ferrarini, A.; Freed, J. H. Modeling the effects of structure and dynamics of the nitroxide side-chain on the ESR spectra of spin labeled proteins. *J. Phys. Chem.*, submitted for publication.

(51) Barone, V.; Polimeno, A. Integrated approaches to modeling ESR observables. *Phys. Chem. Chem. Phys*, in press.

(52) Freed, J. H. *J. Chem. Phys.* **1977**, *66*, 4183−4199.

(53) Choy, W.-Y.; Kay, L. E. *J. Biomol. NMR* **2003**, *25*, 325−333.

(54) (a) Kay, L. E.; Torchia, D. A.; Bax, A. *Biochemistry* **1989**, *28*, 8972−8979. (b) Pawley, N. H.; Wang, C.; Koide, S.; Nicholson, L. K. *J. Biomol. NMR* **2001**, *20*, 149−165.

(55) Polimeno, A.; Moro, G. J.; Freed, J. H. *J. Chem. Phys.* **1995**, *104*, 1090−1104.

(56) Lin, W. J.; Freed, J. H. *J. Phys. Chem.* **1979**, *83*, 379−401.

(57) (a) Bremi, T.; Bruschweiler, R. *J. Am. Chem. Soc.* **1997**, *119*, 6672. (b) Lienin, S. F.; Bremi, T.; Brutsher, B.; Bruschweiler, R.; Ernst, R. R. *J. Am. Chem. Soc.* **1998**, *120*, 9870.

(58) Dingemans, T.; Photinos, D. J.; Samulski, E. T.; Terzis, A. F.; Wutz, C. *J. Chem. Phys.* **2003**, *118*, 7046−7061.

(59) Blackledge, M. *Prog. Nucl. Magn. Reson. Spectrosc.* **2005**, *46*, 23−61.

(60) Prompers, J. J.; Bruschweiler, R. *J. Am. Chem. Soc.* **2001**, *123*, 7305−7313.

(61) Prompers, J. J.; Bruschweiler, R. *J. Am. Chem. Soc.* **2002**, *124*, 4522−4534.

(62) Prompers, J. J.; Bruschweiler, R. *Proteins: Struct., Funct., Genet.* **2002**, *46*, 177−189.

(63) Bernando, P.; Fernandes, M. X.; Jacobs, D. M.; Feibig, K.; de la Torre, J. G.; Pons, M. *J. Biomol. NMR* **2004**, *29*, 21−35.

(64) Lindorff-Larsen, K.; Best, R. B.; DePristo, M. A.; Dobson, C. M.; Vendruscolo, M. *Nature* **2005**, *433*, 128−132.